



Citation for published version:

Palomar, I, Barluenga, G, Ball, R & Lawrence, R 2019, 'Laboratory characterization of brick walls rendered with a pervious lime-cement mortar', *Journal of Building Engineering*, vol. 23, pp. 241-249.
<https://doi.org/10.1016/j.jobe.2019.02.001>

DOI:

[10.1016/j.jobe.2019.02.001](https://doi.org/10.1016/j.jobe.2019.02.001)

Publication date:

2019

Document Version

Peer reviewed version

[Link to publication](#)

Publisher Rights

CC BY-NC-ND

University of Bath

General rights

Copyright and moral rights for the publications made accessible in the public portal are retained by the authors and/or other copyright owners and it is a condition of accessing publications that users recognise and abide by the legal requirements associated with these rights.

Take down policy

If you believe that this document breaches copyright please contact us providing details, and we will remove access to the work immediately and investigate your claim.

Manuscript Details

Manuscript number	JOBE_2018_1493_R1
Title	Laboratory characterization of brick walls rendered with a pervious lime-cement mortar
Article type	Research Paper

Abstract

A laboratory study investigating important thermal retrofitting solutions for simple and double (cavity) brick walls is presented. Test walls were modified using materials of current interest including an external pervious lime-cement mortar render and insulation board prior to evaluation. Laboratory simulations of steady-state winter and summer scenarios were performed using apparatus comprising two opposing climate chambers. Temperature, relative humidity and heat flux rate were monitored with surface sensors every 10 minutes until stabilization on each wall type, retrofitting solution and climate scenario. The temperature and relative humidity profiles, heat flux, surface temperature difference, thermal conductance, condensation risk and stabilization times were assessed. Comparisons between simple and double (cavity) brick walls showed significant differences and a high condensation risk in the non-ventilated air cavity of the double wall. The pervious lime-cement mortar render enhanced substantially the thermal performance of the single wall although increased the condensation risk of the double (cavity) wall. As expected, the insulation layer reduced the thermal conductance of the wall, although the improvement in a summer scenario was considerably lower than in winter. The different performance observed between winter and summer steady-state conditions emphasized the importance of the heat and mass transfer coupling effect. Therefore, this work proves that effective retrofitting depends on materials, wall layouts and climate conditions. These experimental results provide essential knowledge about assessing the effects of common retrofitting solutions especially under hot-dry summer scenarios.

Keywords	Brick walls; Pervious mortar; Retrofitting; Thermal performance; Heat and moisture transfer.
Taxonomy	Construction, Concrete (Composite Building Material)
Manuscript category	Building materials
Corresponding Author	Irene Palomar
Corresponding Author's Institution	University of Alcalá
Order of Authors	Irene Palomar, Gonzalo Barluenga, Richard Ball, Mike Lawrence
Suggested reviewers	Maria Stefanidou, Laia Haurie

Submission Files Included in this PDF

File Name [File Type]

Cover letter_JBE_2018 (R1).docx [Cover Letter]

Response_JBE_2018 (R1).docx [Response to Reviewers]

Lab charact brick walls render PLCM (REV_Marked).docx [Revised Manuscript with Changes Marked]

Highlights_JBE_2018.docx [Highlights]

Lab charact brick walls render PLCM (R1).docx [Manuscript File]

To view all the submission files, including those not included in the PDF, click on the manuscript title on your EVISE Homepage, then click 'Download zip file'.

Department of Architecture
University of Alcala
C/ Santa Úrsula 8 – 28801
Alcalá de Henares (Spain)

Journal of Building Engineering
Elsevier B.V. (Corporate Office)
Radarweg 29
Amsterdam 1043 NX, Netherlands

January 28th, 2019

Dear Professor de Brito,

We are grateful for the opportunity to resubmit for possible publication in Journal of Building Engineering the revised version of JOBE_2018_1493, authored by I. Palomar, G. Barluenga, R.J. Ball, and M. Lawrence, entitled "Laboratory characterization of brick walls rendered with a pervious lime-cement mortar".

We have made all the changes suggested by the reviewers and we have tried to answer all the queries addressed in their comments.

We thank the two reviewers for providing thoughts and comments that have improved this manuscript. They gave us clear guidance and positive critiques. All of the reviews indicated that the paper contained material suitable for the journal and would be of interest for the readers and that it was worthy of publication.

Yours sincerely,

Dr. Irene Palomar
University of Alcala (Spain)

Ref.: JOBE_2018_1493

Title: Laboratory characterization of brick walls rendered with a pervious lime-cement mortar
Journal of Building Engineering

Response to Reviewers' comments:

Reviewer #1:

We thank the reviewer for providing thoughts and comments that have improved this manuscript.

Comment 1. (Table 1). The reviewer suggests to check the water vapor diffusion resistance factors of some materials. The authors have reviewed it, as suggested by the reviewer. Concerning the values of the three bricks, they were provided by the manufacturer (Declaration of Performance – DoP). These values are tabulated from UNE-EN 1745 (Table A.1 – footnote: high density clay masonry units for exterior walls). This reference was added in the text [Ref#37]. On the other hand, the gypsum plaster thermo-physical properties were experimentally characterized. The values were also checked.

Comment 2. (Time to reach steady-state). The reviewer states that the time to reach the steady state in whole system should be explained. Based on the experimental results (Table 3), it was observed that the time to reach steady-state depends on the wall type, retrofitting solutions and climate scenario. For example, RH values of single brick walls stabilizes the last in summer scenario. However, T values stabilize the last for double (cavity) walls in both climate scenarios. As suggested by the reviewer, these results have been highlighted and a sentence was included in the text (Page 10): “It was observed that the time to reach a steady-state regime depends on the wall type, retrofitting solutions and climate scenario (Table 2 and 3). The single brick walls took at least 18 hours to stabilize RH in summer scenario. On the other hand, only REF(S)+X+R showed a similar behaviour (14 hours) in winter. T values, which stabilized the last in the case of double cavity brick walls, required at least 12 hours in all the climate scenarios.”

Reviewer #2:

The authors are very thankful to the reviewer for the valuable comments and contributions.

Laboratory characterization of brick walls rendered with a pervious lime-cement mortar

I. Palomar ^{a,1}, G. Barluenga ^a, R.J. Ball ^b, M. Lawrence ^b

^a Department of Architecture, University of Alcalá, Spain

^b BRE Center for Innovative Construction Materials, Department of Architecture & Civil Engineering, University of Bath, UK

ABSTRACT

A laboratory study investigating important thermal retrofitting solutions for simple and double (cavity) brick walls is presented. Test walls were modified using materials of current interest including an external pervious lime-cement mortar render and insulation board prior to evaluation. Laboratory simulations of steady-state winter and summer scenarios were performed using apparatus comprising two opposing climate chambers. Temperature, relative humidity and heat flux rate were monitored with surface sensors every 10 minutes until stabilization on each wall type, retrofitting solution and climate scenario. The temperature and relative humidity profiles, heat flux, surface temperature difference, thermal conductance, condensation risk and stabilization times were assessed. Comparisons between simple and double (cavity) brick walls showed significant differences and a high condensation risk in the non-ventilated air cavity of the double wall. The pervious lime-cement mortar render enhanced substantially the thermal performance of the single wall although increased the condensation risk of the double (cavity) wall. As expected, the insulation layer reduced the thermal conductance of the wall, although the improvement in a summer scenario was considerably lower than in winter. The different performance observed between winter and summer steady-state conditions emphasized the importance of the heat and mass transfer coupling effect. Therefore, this work proves that effective retrofitting depends on materials, wall layouts and climate conditions. These experimental results provide essential knowledge about assessing the effects of common retrofitting solutions especially under hot-dry summer scenarios.

KEYWORDS

Brick walls; Pervious mortar; Retrofitting; Thermal performance; Heat and moisture transfer.

¹ Corresponding author. Departamento de Arquitectura. Escuela de Arquitectura, Universidad de Alcalá, C. Santa Úrsula, 8. Alcalá de Henares, 28801 Madrid, Spain. Tel.: +34 918839239; fax: +34 918839246 - *E-mail address*: irene.palomar@uah.es (I.Palomar)

1 Introduction

Existing dwelling buildings are part of a large building stock characterized by a large energy consumption, according to current energy efficiency standards [1, 2]. In the case of Spain, around 70% of the dwelling stock was built before the first national energy efficiency regulation was put into force in 1979, and 45% was built between 1960 and 1980 [3]. Due to its low energy efficiency, the residential sector is responsible for over 20% of the total energy consumption in Spain [4]. Thus, energy efficiency improvement has become a main concern and effective retrofitting techniques and materials are required.

Retrofitting this dwelling stock, which includes historical and traditional buildings, is a balance among reducing energy consumption, improving long-term building performance and satisfying today's functional requirements [5]. The most common (and cheapest) retrofitting solution for those buildings is an External Thermal Insulation Composite System (ETICS) [2]. However, some issues arise due to the embodied energy increase of traditional walls [6] and its low adaptability to specific insulation thickness and hygrothermal performance [7] that could produce moisture accumulations and organic growth in cold climates [8] and overheating in summertime [9]. On the other hand, façade retrofitting often requires the substitution of deteriorated traditional mortars, which becomes an opportunity to fulfill the nowadays building requirements through the design of new mortar coatings [10, 11, 12, 13]. Considering this, new pervious lime-cement mortars (PLCM) with short cellulose fibers (CF) have been designed to improve thermal and acoustic properties, fulfilling conservation, aesthetic, structural, service-life and construction issues [14, 15]. The main characteristic of PLCM is the lack of fine aggregate particles that creates an interconnected void network where spherical aggregate particles are surrounded by a shell of lime-cement paste and CF [16].

According to the literature [17], brick wall façades of those residential buildings can have one or two brick layers. Double walls were traditionally built with an intermediate non-ventilated air cavity. Due to the 70's energy crisis, a thermal insulation layer of 30-40 mm was typically incorporated between the brick layers, filling the air cavity. Before 1960, one layer brick walls were a common solution, using solid bricks, and lately 360 mm perforated bricks or even 120 mm hollow bricks.

As the new energy efficiency regulations come into force [1, 5], many brick wall facades were retrofitted with different types of renders, achieving various levels of effectiveness depending on the wall typology and climate scenario. Some studies reproduce common typologies and climate conditions, focusing on factors affecting thermal performance of lime or cement mortars, such as moisture content dependency [18, 19], the interface phenomena in a multiple layer wall [20] or the overestimation of traditional materials and wall properties, due to a lack of experimental data for computer models [21]. However, these results cannot be extrapolated to

other climate conditions as those characterized by high seasonal variations, large diurnal daily ranges and high temperature and low relative humidity on summer days, which are typical of Southern Europe's climate [22], since operating conditions affect the thermal performance of standard and retrofitted walls [6].

The hygrothermal performance of building materials and façade walls can be studied using mathematical and computer models simulating the coupled effect of heat and moisture transfer through multilayer walls [23, 24, 25]. However, these algorithms require reliable material properties from laboratory characterization [26] or involve a long-term monitoring to ensure reliability and overestimate pre-standard buildings performance [27]. Other alternative methods such as outdoor test cells or on-site assessment methods have been reported, which allow consideration of dynamic boundary conditions [28, 29]. Laboratory simulation tests have also been widely used, creating "artificial on-site conditions" with climatic chambers and reproducing either quasi steady-state or dynamic scenarios [7, 30, 31, 32, 33]. Considering both the full-scale and laboratory tests, climate scenarios can be easily applied to any wall layout in the laboratory-controlled conditions to estimate its hygrothermal behavior [34]. Only few studies used a complete approach that included laboratory tests, outdoor test cells, dynamic identification techniques, model calibration, simulation and full-scale building monitoring [35].

This paper presents an experimental program aimed to investigate the effect of a pervious lime-cement mortar render (PLCM) with and without an insulation board for thermal retrofitting of simple and double (cavity) brick walls. Winter and summer steady-state scenarios were simulated using two climatic chambers applied on both sides of the test walls with and without rendering. Temperature, relative humidity and heat flux were monitored. The effectiveness of the retrofitting solution for each wall type, retrofitting solution and climate scenario was assessed.

2 Experimental program

Two wall types, simple and double (cavity) brick walls, two retrofitting solutions including pervious lime-cement mortars (PLCM) and two climate scenarios, steady state winter and summer, were experimentally characterized. The walls and scenarios used in this study reproduce common constructive typologies and climate conditions characterized by high seasonal variations and high temperature and low relative humidity on summer. Two climate chambers were placed opposite one to another on each side of the testing wall to simulate indoor and outdoor conditions. Temperature, relative humidity and heat flux sensors were used to monitor hygrothermal parameters and the measurements were recorded every 10 minutes for at least 24 hours after steady-state conditions were reached. Temperature (T) and relative humidity (RH) profiles, density of heat flux rate (HF), surface temperature difference (ΔT), thermal conductance (Λ), condensation risk (CR) and

stabilization time (t_s) were analyzed. The experimental results were used to compare the different brick walls, retrofitting solutions and climate scenarios.

2.1 Materials

The materials used in the study were:

- Three clay bricks (Category II, HD):
 - vertically perforated bricks (VPB) of 215 x 102.5 x 65 mm,
 - frogged bricks (FB) of 215 x 102.5 x 65 mm,
 - solid bricks (SB) of 215 x 102.5 x 35 mm.
- Four binders:
 - an air lime class CL 90-S,
 - a white cement CEM I 52.5 R –SR5,
 - a cement type CEM II/B-V/32.5R,
 - a one coat gypsum plaster class B4/20/2.
- Two aggregates: a siliceous sand (0-4 mm) and a gap-graded limestone sand (2-3 mm).
- Short cellulose fibers of length 1 mm - Fibracel® BC-1000 ($\varnothing 20\mu\text{m}$) - supplied by Omya Clariana S.L.
- Rigid insulation board of polyisocyanurate foam and low emissivity foil facings (X) of 50 mm.

The binder materials were used to produce a retrofitting render (R), a Plaster (P) and a Joint mortar (J), prepared as follows:

- Retrofitting render (R): Pervious lime-cement mortar (PLCM) with gap-graded limestone sand (1:1:6 by volume lime/cement/sand ratios), cellulose fibres (1.5% of the total dried mortar's volume) and 0.94 water to binder ratio (w/b). This mixture was selected out of twelve evaluated in a previous study due to the particular suitability for external rendering when considering the technical, functional and performance requirements [14]. The use of cellulose fibers in PLCM improved the thermal and acoustic performance - the lowest thermal conductivity coefficient and the highest noise reduction was observed from a previous study as both paste thickness and active void size were modified [16].
- Plaster (P): A one coat gypsum plaster with w/b = 0.45
- Joint mortar (J): Cement mortar with continuous siliceous sand (1:6 by volume) and w/b = 1

Table 1 summarizes some materials' properties as bulk density (ρ), moisture-dependent water vapor diffusion resistance factor (μ), thermal conductivity (λ), specific heat (c_p) and thermal diffusivity (α). Thermal diffusivity (α) was calculating according to Eq. (1) [36]:

$$\alpha = \frac{\lambda}{\rho \cdot c_p} \quad (1)$$

where λ is the thermal conductivity of the material, ρ is bulk density and c_p specific heat.

The retrofitting render (R) was previously characterized and showed a suitable thermal and acoustic performance [14, 15, 16]. The gypsum plaster thermo-physical properties were experimentally characterized. Nominal properties for bricks [37] and insulation board provided by the manufacturers were considered, although slight differences can be expected due to the effect of temperature, moisture and aging [38].

2.2 Façade brick wall layouts

Five wall configurations, three single walls and two double (cavity) walls, were fabricated. Fig. 1 shows the 450 x 440 mm brick wall cross-sections.

The reference single wall (REF(S)) was built with one 103 mm thick layer of vertically perforated bricks (VPB) and a joint cement mortar (J), while the reference double (cavity) wall (REF(D)) was built with two layers, 35 mm solid bricks (SB) and 103 mm frogged bricks (FB), with a 40 mm non-ventilated air cavity (A) in between. The interior side of both walls was coated with 15 mm gypsum plaster (P).

Then, the external side of both walls was rendered with a 25 mm pervious lime-cement mortar (R), named REF(S)+R and REF(D)+R respectively. The single wall was also retrofitted combining a 50 mm thick thermal insulation board (X) with the pervious lime-cement render (R), noted as REF(S)+X+R. A polyisocyanurate (PIR) insulation panel was selected to reduce insulation thickness while complying with energy efficiency standards [39, 40]. Besides, PIR has the best fire resistance among foam plastics [39].

The design thermal conductance (Λ_c) of the wall layouts was calculated according to Eq. (2) [36]:

$$\Lambda_c = \frac{1}{\sum_j \frac{d_j}{\lambda_j}} \quad (2)$$

where λ is the thermal conductivity and d is the thickness of each layer (j) in Table 1.

2.3 Experimental methods

Fig. 2 shows the experimental setup designed for this study. The walls were built inside a plywood framework, sealed and thermally isolated with polyisocyanurate foam to allow a one-dimensional heat and moisture flux. Samples were stored under laboratory conditions at $22 \pm 2^\circ\text{C}$ and $60 \pm 10\%$ RH until testing. The framework with the wall was then placed between two climate chambers simulating the effect of different climate conditions on the walls. Temperature (T) and relative humidity (RH) were set using two TAS MTCL-135 climate

chambers with HMI Control Systems which was used to produce heat and moisture flux that simulated winter and summer scenarios. The water vapor density (v) for each scenario was estimated according to ISO 13788 [40]. The interior conditions were set at 23°C and 50 ±5% RH ($v = 0.0103 \pm 0.001 \text{ kg/m}^3$) and the exterior conditions were 12°C, 80±5% RH ($v = 0.0085 \pm 0.0005 \text{ kg/m}^3$) for winter and 31°C, 40±5% RH ($v = 0.0128 \pm 0.002 \text{ kg/m}^3$) for summer. These conditions were selected to simulate climates with high seasonal variations and high temperature and low RH in summer.

K type thermocouples and relative humidity sensors (HIH4000) were used to monitor the interior of the chambers and the surfaces of all the layers of the walls at 10 minute intervals. A heat flux sensor (HFP01 by Hukseflux) was placed in the interior side of the walls. The operational error in the heat flux meter (HFM) was calculated as 10% to 22%, according to ISO 9869 [42]. Temperature (T), relative humidity (RH) and density of heat flux rate (HF) were monitored on the walls and the results were analyzed after a steady-state regime was reached. Afterwards, laboratory-experimental thermal conductance (Λ), risk of surface and interstitial condensation (CR) and transition time (t_s) were calculated and used to compare single and double walls with and without retrofitting solutions in winter and summer scenarios. Laboratory-experimental thermal conductance (Λ) of the wall layouts was estimated using the ratio between the mean density of heat flow rate (HF) and mean temperature difference between the interior ($T_{s,i}$) and exterior ($T_{s,e}$) surfaces after a steady-state regime was reached over a long enough period of time [41,42].

3 Experimental results

Two wall types, simple and double cavity brick walls, two retrofitting solutions with an exterior pervious lime-cement mortar render with and without an insulation board, and two steady-state climate scenarios, winter and summer, were experimentally characterized.

3.1 Laboratory characterization of simple brick walls

Temperature (T) and relative humidity (RH) cross-sections of the single walls in steady-state winter and summer scenarios are plotted in Fig. 3. It can be observed that the addition of exterior pervious lime-cement mortar render and an insulation board produced different effects.

In the winter scenario, the temperature difference (ΔT) for the brick layer (W_1) was 6.45 °C in the reference single wall REF(S), whereas ΔT were 3.95 and 0.52 °C for rendered (REF(S)+R) and insulated (REF(S)+X+R) single walls respectively. The highest RH values were found on the exterior pervious lime-cement mortar

render (R) both in REF(S)+R and REF(S)+X+R walls. However, RH was lower than 100% and there was no surface or interstitial condensation in any single wall in the winter scenario.

In the summer scenario, the addition of exterior pervious lime-cement mortar render (R) reduced the temperature difference of the brick layer (W_1) from 4.20 °C to 2.47 °C. In addition, the interior plaster (P) also showed lower temperatures. When an insulation board (X) was added, its temperature difference was 5.68 °C and almost zero in the other layers. RH cross-sections showed similar values for both REF(S) and REF(S)+R. On the other hand, the addition of an insulation board (X) increased RH between W_1 and X layers, although no surface or interstitial condensation was recorded.

3.2. Laboratory characterization of double (cavity) brick walls

Fig. 4 shows temperature (T) and relative humidity (RH) cross-sections of the double (cavity) walls measured in steady-state winter and summer scenarios, showing the effect of a non-ventilated air cavity (REF(D)) and an exterior pervious lime-cement mortar render (REF(D)+R).

REF(D) temperature cross-section in the winter steady-state scenario showed that the interior brick layer (W_2), the non-ventilated air cavity (A) and the exterior brick layer (W_3) had temperature differences (ΔT) of 1.39, 4.21 and 3.53 °C, respectively. In the case of REF (D)+R, the render (R) showed a ΔT of 2.26 °C and halved the temperature difference of the non-ventilated air cavity to 2.20 °C. The brick layers (W_2 and W_3) and plaster (P) had similar temperatures in both walls. The RH cross-section of REF(D) showed a high relative humidity in the air cavity (A) and interstitial condensation occurred. Nevertheless, no surface condensation in winter conditions was recorded. The same happened on the rendered wall, REF(D)+R: interstitial condensation occurred, especially in the exterior brick layer (W_3), but no surface condensation was recorded.

In the summer scenario, the interior brick layer (W_2), the non-ventilated air cavity (A) and the exterior brick layer (W_3) had a temperature differences (ΔT) of 1.95, 1.54 and 4.38 °C, respectively. Therefore, the non-ventilated air cavity (A) had less effect on temperature cross-section in summer than in winter, whereas the external brick layer (W_3) showed the higher thermal difference. The addition of exterior PLCM render (R) reduced the temperature difference of the interior brick layer (W_2) and the non-ventilated air cavity (A) to one half and the external brick layer (W_3) to one third which was the lowest recorded in this layer. The render layer had a ΔT of 3.55 °C, which corresponded to 44% of the total temperature difference while in the winter scenario a temperature difference of only 22% was reached. Therefore, the rendering produced a larger improvement on double walls in summer than in winter. RH of REF(D) was also different in summer than in the winter scenario, as the brick layer (W_3) condensed water in summer. Moreover, the addition of the rendering (REF(D)+R) extended the area affected by interstitial condensation to the air cavity (A) and the external brick

layer (W_3). However, this cannot be considered a problem because the condensed water can easily evaporate in summer conditions.

4 Analysis and discussion

The laboratory data was used to compare the different brick walls, retrofitting solutions and scenarios. Density of heat flux rate (HF), surface temperature difference (ΔT), thermal conductance (Λ), stabilization time ($t_{s, HF}$; $t_{s, \Delta T}$) and condensation risk (CR) during steady-state winter and summer conditions were analyzed and the experimental results summarized in Table 2. One-dimensional heat and moisture flux through the walls can be assumed for both steady-state scenarios. In winter, the heat and moisture transfer occurred from the inside to the outside (outwards), while in summer, the flux was from the outside to the inside (inwards).

4.1 Effect of the non-ventilated air cavity on the wall performance

Table 2 shows the laboratory measurements of density of heat flux rate (HF) and surface temperature difference (ΔT) of single and double walls. It can be observed that the ΔT value reached an asymptotic situation earlier than HF ($t_{s, \Delta T} < t_{s, HF}$). The larger difference in double walls can be partially attributed to the water condensed in the non-ventilated air cavity (Fig. 4). HF stabilization occurred after the moisture flow ended, due to the heat and mass transfer coupling effect.

The effect of the non-ventilated air cavity on the wall performance can be evaluated comparing the heat flux (HF), surface temperature difference (ΔT), thermal conductance (Λ), stabilization time ($t_{s, \Delta T}$; $t_{s, HF}$) and condensation risk (CR) during steady-state winter and summer conditions (Table 2). Double brick walls reduced the heat flux of single walls in both scenarios by almost three times. This can be explained by the low thermal conductivity of the still air in the non-ventilated air cavity (A). In addition, the surface temperature difference was around 1°C higher in the double compared to the simple wall. Although the non-ventilated air cavity (A) reduced significantly the thermal conductance, a high condensation risk was observed in all scenarios and the air cavity would require drainage. Concerning the stabilization time of HF, REF(D) doubled the time of REF(S) to stabilize in winter, whereas both walls stabilized almost simultaneously in summer. The differences of $t_{s, HF}$ can be attributed to the condensed water and moist air in the non-ventilated air cavity in winter and summer which would modify the materials' specific heat and thermal conductivity, increasing heat storage [43].

4.2 Assessment of the retrofitting solutions

In this section, the effect of a pervious lime-cement mortar render (R) and an insulation board (X) on single and double brick walls was evaluated.

4.2.1 Effect of pervious lime-cement mortar render (R)

Rendering the simple and double brick walls with a pervious lime-cement mortar produced two effects related to the heat and moisture transfer. On one hand, the insulation capacity of the mortar reduced the measured thermal conductance (Λ) (Table 2). This reduction was larger in the simple wall compared to the double wall and also in the summer conditions compared to the winter conditions. In addition, the rendered double wall REF(D)+R showed a similar thermal conductance as the insulated single wall REF(S)+X+R in the summer scenario.

The second effect was related to the low vapor permeability of the mortar which modified moisture transfer. The consequences on double brick walls can be summarized as an increase of condensation inside the non-ventilated air cavity and an extension of the layers affected by interstitial condensation risk (Fig.4).

The combined effect of the render on the heat and moisture transfer also delayed the heat flux stabilization time ($t_{s,HF}$) in all scenarios and wall types, except for the double wall in winter conditions. REF(D)+R in summer conditions showed the highest heat flux stabilization time. The explanation can be found on its insulation capacity and low permeability jointly with its thermal inertia, as the moisture content modified specific heat and increased heat storage of building materials [43].

Accordingly, the incorporation of the render layer on the external side of the walls produced a reduction of the energy needed to keep the interior conditions which would mean lower energy consumption for air conditioning. It would also reduce the thermal variations of the brick layers which would improve their dimensional stability, reducing the cracking risk of the wall under severe climate variations and would improve wall durability [9]. However, the thermal difference between render and brick wall would require a good adherence between the mortar and the brick layer.

4.2.2 Effect of the insulation board (X)

The incorporation of a thermal insulation board, jointly with the mortar render, on the exterior side of the single wall as an improved retrofitting solution produced a significant reduction of heat flux (Table 2), as expected [44]. However, the overall improvement depended on the climate conditions: the thermal conductance measured (Table 2) in the winter scenario was half of the design value (Fig. 1), remarkably better than

expected, while in the summer scenario the value was doubled. Therefore, the effect of the insulation board was strongly reduced in summer conditions. Those results agree with the literature: differences between experimental and design values when insulation was included [21] and those differences are larger in summer conditions than in winter [39].

A secondary effect of the insulation board was the vapor barrier effect due to its extremely low vapor permeability. This property significantly reduced heat flux stabilization time, especially in winter scenario, reaching a value similar to the rendered double wall (REF(D)+ R) in winter which was highly affected by condensation. This can be related to the reduction of vapor transfer jointly with the flux and moisture direction in each case (outwards in winter and inwards in summer), and it could lead to an increased risk of damage in the render layer in winter and the plaster in summer due to moisture accumulation and of interfacial mechanisms [20].

4.3 Temperature (T), relative humidity (RH) and heat flux (HF) stabilization time

Stabilization began in the external layers and was reached later in the internal layers, both in winter and summer scenarios, except for the non-ventilated air cavity due to its lack of thermal inertia. It was observed that the time to reach a steady-state regime depends on the wall type, retrofitting solutions and climate scenario (Table 2 and 3). The single brick walls took at least 18 hours to stabilize RH in summer scenario. On the other hand, only REF(S)+X+R showed a similar behaviour (14 hours) in winter. T values, which stabilized the last in the case of double cavity brick walls, required at least 12 hours in all the climate scenarios.

In general, single walls stabilized slightly faster in winter than in summer. When the three single wall layouts were compared (Table 3), REF(S)+X+R exhibited the lower stabilization time of HF, followed by REF(S) and REF(S)+R. Consequently, REF(S)+X+R took less time to reach an equilibrium compared to other single walls. In double walls (Table 3), REF(D)+R showed the longest stabilization time in summer for both T and HF, but not for RH. However, this wall was the fastest to stabilize HF in winter, with stabilization times shorter than those obtained for single walls.

Regarding the three parameters evaluated, RH stabilized before T and HF, with the exception of REF(S) in summer and the thermally insulated single wall in both scenarios, REF(S)+X+R, which showed the opposite. In this case (REF(S)+X+R), the delay on RH values in Table 3 corresponded to insulation-render interlayer (X-R) in winter and to plaster-internal brick interlayer (P -W₁) in summer. As far as there were peaks on RH and not on temperature stabilization time data (Table 3), it can be assumed that this change was due to the vapor barrier effect of the insulation board. In double walls, HF always stabilized before T. The heat and mass transfer coupling effect can explain why heat flow stabilization occurred after the moisture flow ended.

4.4 Effective brick wall retrofitting in different climate scenarios

The experimental results pointed out that the simple and double brick walls and retrofitting solutions behaved different in winter and summer scenarios, which agrees with previous studies [45]. Thermal conductance measured in the laboratory tended to be higher in winter than in the summer scenario and different from the design values. Heat flux stabilization time was longer in summer than in winter scenario. The effect of climate conditions also depended on the layers affected by interstitial condensation in double brick walls, due to a heat and moisture transfer coupling effect which would modify the materials' specific heat, thermal conductivity and heat storage capacity [43]. It would be a positive effect in summer (inwards heat and moisture transfer) due to the increase of thermal capacity, but a negative effect in winter (outwards transfer) due to the increase of thermal conductivity.

The use of an external insulation board on simple brick walls reduced the heating demand significantly in winter. However, the insulation capacity depended on the climate conditions and was strongly reduced in summer, as reported previously [39]. On the other hand, the use of the pervious lime-cement mortar render on the external side of the double brick walls produced a reduction of the cooling energy needed to maintain the interior conditions in summer which would mean less energy consumption in air conditioning [47, 34]. Therefore, the effectiveness of a retrofitting solution depends on both the material properties and the climate conditions.

Consequently, heating and cooling demand would be underestimated if the heat and moisture coupling effect is not considered. This is in agreement with other authors who highlighted the need of different strategies than thermal insulation to enhance the thermal performance of buildings in climates with a hot summer [46].

5 Conclusions

This paper presents a laboratory characterization of two wall types, simple and double (cavity) brick walls, two retrofitting solutions, a pervious lime-cement mortar render with and without an insulation board, and two climate scenarios, steady state winter and summer simulated using two climate chambers. The experimental program measured temperature, relative humidity (RH) and heat flux rate (HF). Laboratory-experimental thermal conductance, surface and interstitial condensation and temperature, RH and heat flux stabilization time were calculated. The main findings of the study are:

- The measured results of experimental thermal conductance were different from the calculated values and depended on the climate conditions.

- The hygrothermal stabilization of the wall occurred first on the outer layers and afterwards in the inner layers. RH stabilized first, then temperature and HF stabilized the last, due to the heat and moisture coupling effect.
- Double (cavity) brick walls showed better thermal performance than simple walls due to the non-ventilated air cavity. However, double brick walls showed a high condensation risk in both winter and summer scenarios and the air cavity would require drainage.
- The use of an exterior pervious lime-cement mortar render (R) improved the thermal performance of both single and double walls, delaying the heat flux stabilization time. Although, it can increase interstitial condensation in double walls due to the render's low vapor permeability.
- The use of an external insulation board (X) improved the thermal performance in winter conditions, significantly reducing the heat flux and, therefore, the energy required for heating. However, the behavior in summer scenario was significantly worse than expected.
- The differences between expected and measured results can be attributed to the effect of moisture transfer on heat transfer and wall thermal properties. Therefore, the effectiveness of a retrofitting solution depends on both the material properties, and the climate conditions.

Acknowledgments

The authors wish to acknowledge the help of Dr Eshrar Latif and Dr Daniel Maskell, and the contribution on the testing preparation of the technical staff of the Engineering & Design Technical Services at the Department of Architecture and Civil Engineering, University of Bath. Some of the components were supplied by Omya Clariana S.L.

Funding

Financial support for this research was provided by the Trainee Research Personnel Mobility Grant (Movilidad PIF-UAH 2015) and Grant for training of Lecturers (FPU-UAH 2013), funded by the University of Alcalá.

Declarations of interest

None

References

- [1] Directive 2010/31/EU of the European Parliament and of the Council of 19 May 2010 on the energy performance of buildings. Official Journal of the European Union, n° L 153, of 18 June 2010
- [2] Ma Z, Cooper P, Daly D, Ledo L (2012) Existing building retrofits: Methodology and state-of-the-art. *Energy Build* 55: 889-902. <https://doi.org/10.1016/j.enbuild.2012.08.018>
- [3] “Owner-occupied dwellings by type and year of construction of the building” (2001) Eurostat database, European Commission, Luxembourg. http://ec.europa.eu/eurostat/web/products-datasets/product?code=cens_01ndpercons. Accessed 10 May 2016
- [4] Pérez-Lombard L, Ortiz J, Pout C (2008) A review on buildings energy consumption information. *Energy Build* 40(3):394-398. <https://doi.org/10.1016/j.enbuild.2007.03.007>
- [5] Webb AL (2017) Energy retrofits in historic and traditional buildings: A review of problems and methods. *Renewable Sustainable Energy Rev* 77:748-759. <https://doi.org/10.1016/j.rser.2017.01.145>
- [6] Kyriakidis A, Michael A, Illampas R, Champis DC, Ioannou I (2018) Thermal performance and embodied energy of standard and retrofitted wall systems encountered in Southern Europe, *Energy* 161: 1016-1027. <https://doi.org/10.1016/j.energy.2018.07.124>.
- [7] Johansson P, Geving S, Hagentoft CE, Jelle BP, Rognvik E, Kalagasidis AS, Time B (2014) Interior insulation retrofit of a historical brick wall using vacuum insulation panels: Hygrothermal numerical simulations and laboratory investigations. *Build Environ* 79:31-45. <https://doi.org/10.1016/j.buildenv.2014.04.014>
- [8] Künzle HM (1998) Effect of interior and exterior insulation on the hygrothermal behaviour of exposed walls. *Mater Struct* 31(2):99 -103
- [9] Gupta R, Gregg M (2018) Assessing energy use and overheating risk in net zero energy dwellings in UK. *Energy Build* 158:897-905. <https://doi.org/10.1016/j.enbuild.2017.10.061>
- [10] Govaerts Y, Hayen R, de Bouw M, Verdonck A, Meulebroeck W, Mertens S, Grégoire Y (2018) Performance of a lime-based insulating render for heritage buildings. *Constr Build Mater* 159:376-389. <https://doi.org/10.1016/j.conbuildmat.2017.10.115>
- [11] Bianco L, Serra V, Fantucci S, Dutto M, Massolino M, (2015) Thermal insulating plaster as a solution for refurbishing historic building envelopes: First experimental results. *Energy Build* 95:86-91. <https://doi.org/10.1016/j.enbuild.2014.11.016>
- [12] Ibrahim M, Biwole PH, Wurtz E, Achard P (2014) A study on the thermal performance of exterior walls covered with a recently patented silica-aerogel-based insulating coating. *Build Environ* 81:112-122. <https://doi.org/10.1016/j.buildenv.2014.06.017>

- [13] Stefanidou M (2014) Cement-based renders with insulating properties. *Constr Build Mater* 65: 427-431. <https://doi.org/10.1016/j.conbuildmat.2014.04.062>
- [14] Palomar I, Barluenga G, Puentes J (2015) Lime–cement mortars for coating with improved thermal and acoustic performance. *Constr Build Mater* 75: 306-314. <https://doi.org/10.1016/j.conbuildmat.2014.11.012>
- [15] Palomar I, Barluenga G (2017) Assessment of lime-cement mortar microstructure and properties by P- and S- ultrasonic waves. *Constr Build Mater* 139:334-341. <https://doi.org/10.1016/j.conbuildmat.2017.02.083>
- [16] Palomar I, Barluenga G (2018) A multiscale model for pervious lime-cement mortar with perlite and cellulose fibers. *Constr Build Mater* 160:136-144. <https://doi.org/10.1016/j.conbuildmat.2017.11.032>
- [17] Terés-Zubiaga J, Martín K, Erkoreka A, Sala JM (2013) Field assessment of thermal behaviour of social housing apartments in Bilbao, Northern Spain. *Energy Build* 67:118-135. <https://doi.org/10.1016/j.enbuild.2013.07.061>
- [18] Pavlík Z, Vejmelková E, Fiala L, Černý R (2009) Effect of moisture on thermal conductivity of lime-based composites. *Int J Thermophys* 30 (6):1999-2014. <https://doi.org/10.1007/s10765-009-0650-y>
- [19] Khan MI (2002) Factors affecting the thermal properties of concrete and applicability of its prediction models. *Build Environ* 37(6): 607-614. [https://doi.org/10.1016/S0360-1323\(01\)00061-0](https://doi.org/10.1016/S0360-1323(01)00061-0)
- [20] De Freitas VP, Abrantes V, Crausse P (1996) Moisture migration in building walls—Analysis of the interface phenomena. *Build Environ* 31(2):99-108. [https://doi.org/10.1016/0360-1323\(95\)00027-5](https://doi.org/10.1016/0360-1323(95)00027-5)
- [21] Walker R, Pavía S (2015) Thermal performance of a selection of insulation materials suitable for historic buildings. *Build Environ* 94(Part 1):155-165. <https://doi.org/10.1016/j.buildenv.2015.07.033>
- [22] Stazi F, Bonfigli C, Tomassoni E, Di Perna C, Munafò P (2015) The effect of high thermal insulation on high thermal mass: Is the dynamic behaviour of traditional envelopes in Mediterranean climates still possible? *Energy Build* 88:367-383. <https://doi.org/10.1016/j.enbuild.2014.11.056>
- [23] Qin M, Belarbi R, Ait-Mokhtar A, Nilsson LO (2009) Coupled heat and moisture transfer in multi-layer building materials. *Constr Build Mater* 23(2): 967-975. <https://doi.org/10.1016/j.conbuildmat.2008.05.015>
- [24] Skujans J, Vulans A, Iljins U, Aboltins A (2007) Measurements of heat transfer of multi-layered wall construction with foam gypsum. *Appl Therm Eng* 27(7):1219-1224. <https://doi.org/10.1016/j.applthermaleng.2006.02.047>
- [25] Bellia L, Minichiello F (2003) A simple evaluator of building envelope moisture condensation according to an European Standard. *Build Environ* 38(3): 457-468. [https://doi.org/10.1016/S0360-1323\(02\)00060-4](https://doi.org/10.1016/S0360-1323(02)00060-4)

- [26] López O, Torres I, Guimarães AS, Delgado JMPQ, de Freitas VP (2017) Inter-laboratory variability results of porous building materials hygrothermal properties. *Constr Build Mater* 156:412-423. <https://doi.org/10.1016/j.conbuildmat.2017.08.184>
- [27] Lucchi E (2017) Thermal transmittance of historical brick masonries: a comparison among standard data, analytical calculation procedures, and in situ heat flow meter measurements. *Energy Build* 134:171-184. <https://doi.org/10.1016/j.enbuild.2016.10.045>
- [28] Jiménez MJ, Porcar B, Heras MR (2009) Application of different dynamic analysis approaches to the estimation of the building component U value. *Build Environ* 44(2):361-367. <https://doi.org/10.1016/j.buildenv.2008.03.010>
- [29] Toman J, Vimrová A, Černý R (2009) Long-term on-site assessment of hygrothermal performance of interior thermal insulation system without water vapor barrier. *Energy Build* 41(1):51-55. <https://doi.org/10.1016/j.enbuild.2008.07.007>
- [30] Latif E, Tucker S, Ciupala MA, Wijeyesekera DC, Newport DJ, Pruteanu M (2016) Quasi steady state and dynamic hygrothermal performance of fibrous Hemp and Stone Wool insulations: Two innovative laboratory based investigations. *Build Environ* 95:391-404. <https://doi.org/10.1016/j.buildenv.2015.10.006>
- [31] Pavlík Z, Černý R (2008) Experimental assessment of hygrothermal performance of an interior thermal insulation system using a laboratory technique simulating on-site conditions. *Energy Build* 40(5): 673-678. <https://doi.org/10.1016/j.enbuild.2007.04.019>
- [32] Moradas PA, Silva PD, Castro-Gomes JP, Salazar MV, Pires L (2012) Experimental study on hygrothermal behaviour of retrofit solutions applied to old building walls. *Constr Build Mater* 35:864-873. <https://doi.org/10.1016/j.conbuildmat.2012.04.138>
- [33] Palumbo M, Lacasta AM, Giraldo MP, Haurie L, Correal E (2018) Bio-based insulation materials and their hygrothermal performance in a building envelope system (ETICS). *Energy Build* 174:147-155. <https://doi.org/10.1016/j.enbuild.2018.06.042>
- [34] Ferrari S, Zanotto V (2013) The thermal performance of walls under actual service conditions: Evaluating the results of climatic chamber tests. *Constr Build Mater* 43: 309-316. <https://doi.org/10.1016/j.conbuildmat.2013.02.056>
- [35] Strachan PA, Vandaele L (2008) Case studies of outdoor testing and analysis of building components. *Build Environ* 43(2):129-142. <https://doi.org/10.1016/j.buildenv.2006.10.043>
- [36] UNE-EN ISO 7345 (1996) Thermal insulation. Psychical quantities and definitions. Spanish Organization for Standardization (AENOR)

- [37] UNE-EN 1745 (2013) Masonry and masonry products - Methods for determining thermal properties. Spanish Organization for Standardization (AENOR)
- [38] UNE-EN ISO 10456 (2007) Buildings materials and products. Hygrothermal properties. Tabulated design values and procedures for determining declared and design thermal values. Spanish Organization for Standardization (AENOR)
- [39] Schiavoni S, D'Alessandro F, Bianchi F, Asdrubali F (2016) Insulation materials for the building sector: A review and comparative analysis. *Renewable Sustainable Energy Rev* 62:988-1011. <https://doi.org/10.1016/j.rser.2016.05.045>
- [40] Pescari S, Tudor D, Tölgyi S, Maduta C (2015) Study concerning the thermal insulation panels with double-side anti-condensation foil on the exterior and polyurethane foam or polyisocyanurate on the interior. *Key Eng. Mater* 660, 2015: 244–248. <https://doi:10.4028/www.scientific.net/KEM.660.244>
- [41] UNE-EN ISO 13788 (2001) Hygrothermal performance of buildings components and buildings elements. Internal surface temperature to avoid critical surface humidity and interstitial condensation. Calculation method. Spanish Organization for Standardization (AENOR)
- [42] BS ISO 9869-1 (2014) Thermal insulation — Building elements — In-situ measurement of thermal resistance and thermal transmittance. Part 1: Heat flow meter method. British Standards Institution (BSI)
- [43] Jerman M, Černý R (2012) Effect of moisture content on heat and moisture transport and storage properties of thermal insulation materials. *Energy Build* 53: 39-46. <https://doi.org/10.1016/j.enbuild.2012.07.002>
- [44] Cabeza LF, Castell A, Medrano M, Martorell I, Pérez G, Fernández I (2010) Experimental study on the performance of insulation materials in Mediterranean construction. *Energy Build* 42(5):630-636. <https://doi.org/10.1016/j.enbuild.2009.10.033>
- [45] Mazzeo D, Oliveti G, Arcuri N (2016) Influence of internal and external boundary conditions on the decrement factor and time lag heat flux of building walls in steady periodic regime. *Appl Energy* 164: 509-531. <https://doi.org/10.1016/j.apenergy.2015.11.076>
- [46] Corrado V, Paduos S (2016) New equivalent parameters for thermal characterization of opaque building envelope components under dynamic conditions. *Appl Energy* 163:313-322. <https://doi.org/10.1016/j.apenergy.2015.10.123>
- [47] Aste N, Leonforte F, Manfren M, Mazzon M, (2015) Thermal inertia and energy efficiency – Parametric simulation assessment on a calibrated case study. *Appl Energy* 145:111-123. <https://doi.org/10.1016/j.apenergy.2015.01.084>

List of figures and tables

Fig. 1 Vertical cross section of wall layouts (Λ_c = designed thermal conductance)

Fig. 2 Experimental setup for climate scenarios simulated using two climate chambers (distance in mm)

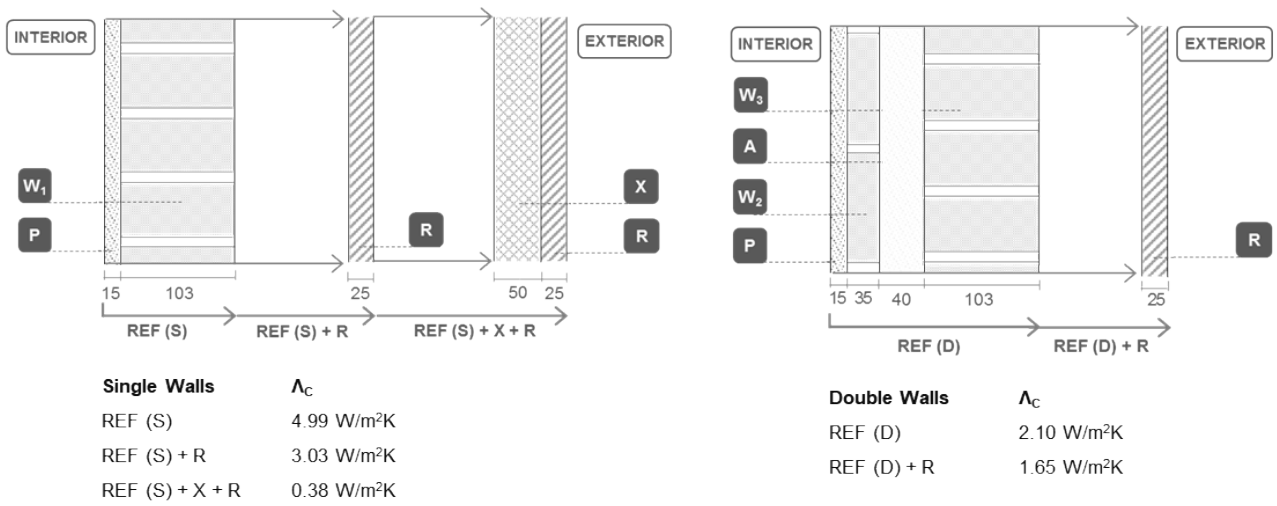
Fig. 3 Temperature and relative humidity steady-state winter and summer scenarios

Fig. 4 Temperature and relative humidity cross-sections of double (cavity) walls in steady-state winter and summer scenarios

Table 1 Materials' Properties

Table 2 Laboratory measured thermal parameters in winter and summer scenarios

Table 3 Temperature, relative humidity and heat flux stabilization time of single and double walls in winter and summer scenarios



A: No ventilated air cavity **R:** Lime-cement mortar **W₁:** Perforated brick layer **W₃:** Froged brick layer
P: One coat universal plaster **X:** PIR insulation board **W₂:** Solid brick layer **Distances in mm**

Fig. 1 Vertical cross section of wall layouts (Λ_c = designed thermal conductance)

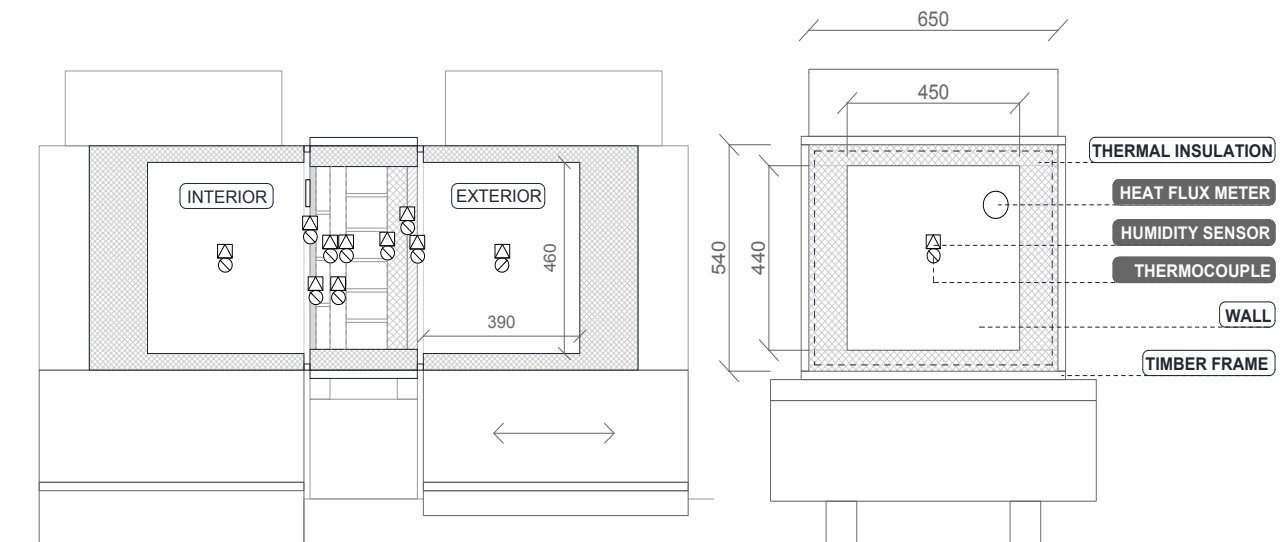


Fig. 2 Experimental setup for climate scenarios simulated using two climate chambers (distance in mm)

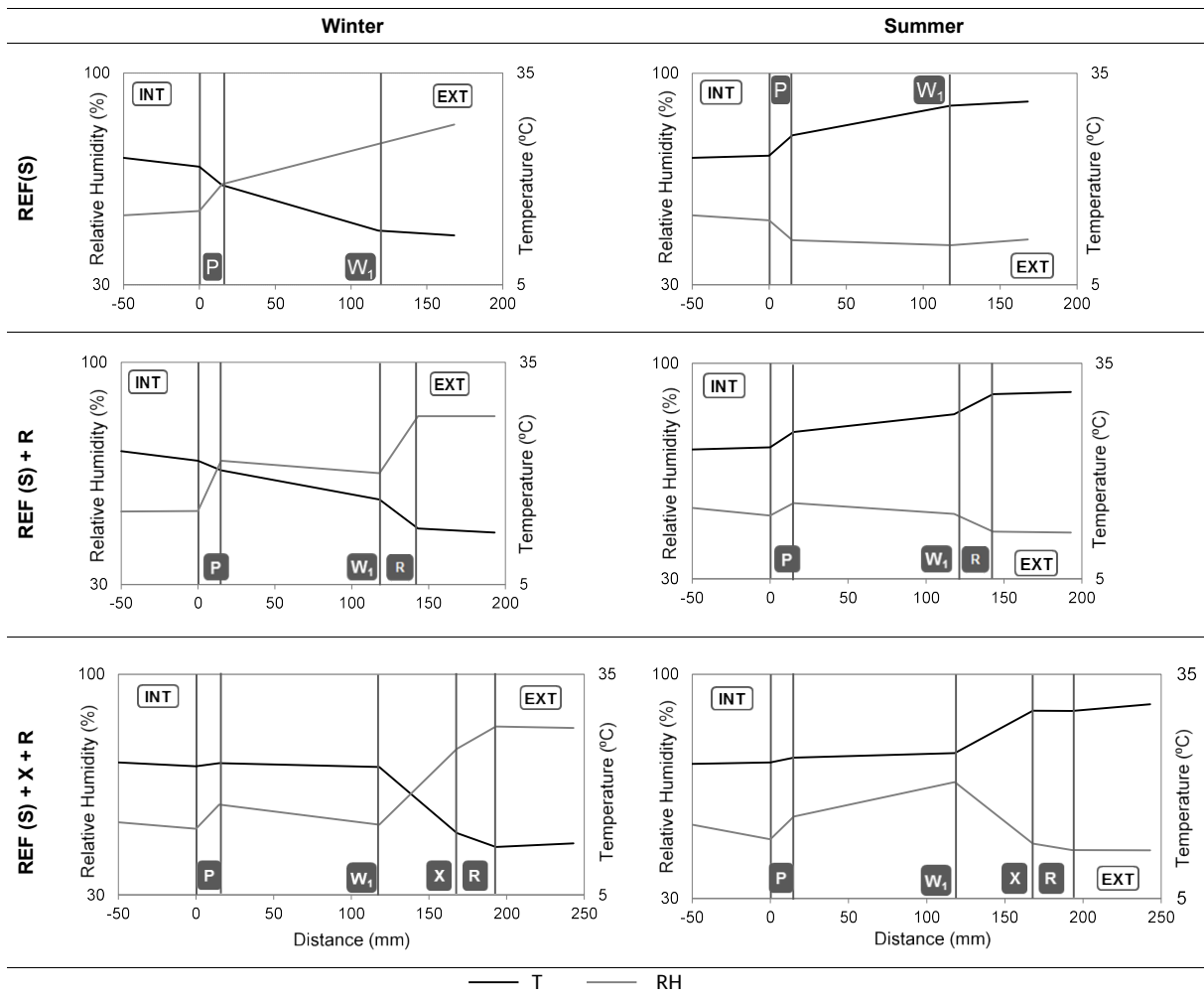


Fig. 3 Temperature and relative humidity cross-section of single walls in steady-state winter and summer scenarios

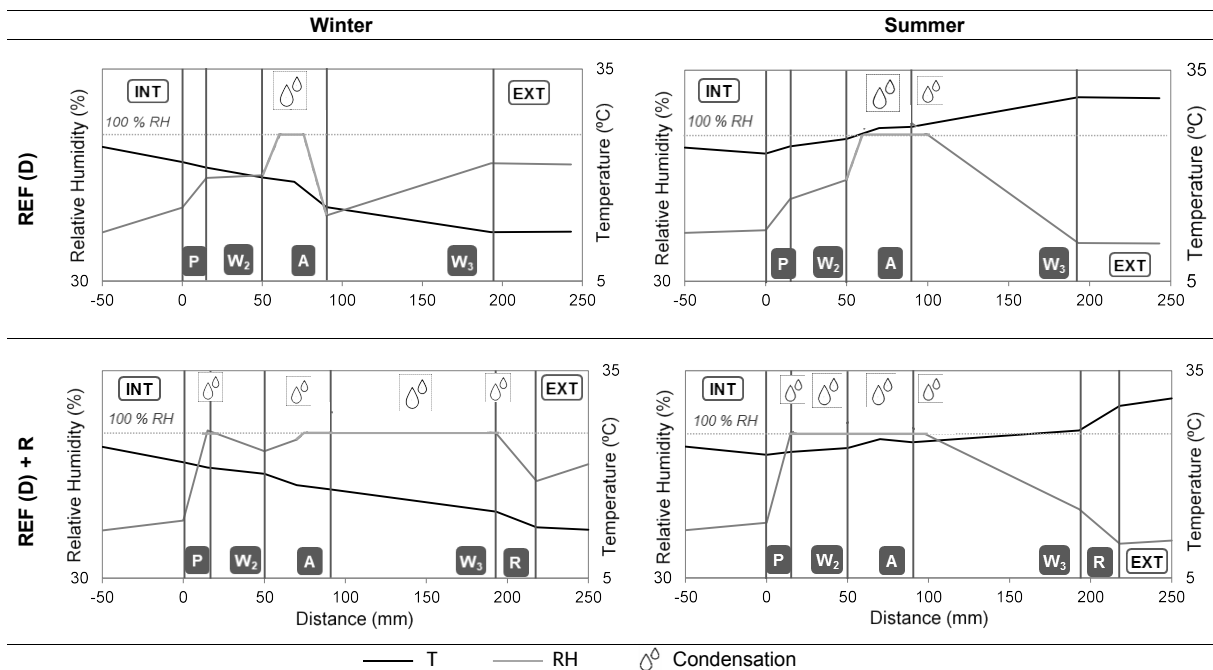


Fig. 4 Temperature and relative humidity cross-section of double walls in steady-state winter and summer scenarios

Table 3 Temperature, relative humidity and heat flux stabilization time of single and double walls in winter and summer scenarios

		REF (S)		REF (S) + R		REF (S) + X+ R		REF (D)		REF (D) + R		
		HF		HF		HF		HF		HF		
		Time (h)		9.00		2.33		8.67		1.67		
		T	RH	T	RH	T	RH	T	RH	T	RH	
WINTER	S _i	h	3.00	1.33	5.50	4.83	4.33	4.00	7.50	7.50	0.67	1.00
	P- W ₁	h	3.50	1.67	9.67	8.00	0.50	4.67	-	-	-	-
	W ₁ - R	h	-	-	10.33	6.33	-	-	-	-	-	-
	W ₁ - X	h	-	-	-	-	2.67	4.00	-	-	-	-
	X - R	h	-	-	-	-	5.33	13.83	-	-	-	-
	P- W ₂	h	-	-	-	-	-	-	9.50	9.33	1.67	10.83
	W ₂ - A	h	-	-	-	-	-	-	11.00	x	8.33	6.67
	A	h	-	-	-	-	-	-	12.33	9.83	3.17	0.67
	A- W ₃	h	-	-	-	-	-	-	13.83	5.67	4.33	3.00
	W ₃ - R	h	-	-	-	-	-	-	-	-	11.50	9.17
	S _e	h	2.00	3.00	6.33	4.33	2.67	3.17	8.33	7.50	7.00	5.33
			HF		HF		HF		HF		HF	
		Time (h)		12.83		6.00		6.67		18.00		
		T	RH	T	RH	T	RH	T	RH	T	RH	
SUMMER	S _i	h	4.50	9.50	6.50	6.00	0.00	0.00	6.50	3.67	12.00	6.00
	P- W ₁	h	7.00	14.50	11.00	17.67	7.83	18.00	-	-	-	-
	W ₁ - R	h	-	-	12.00	10.33	-	-	-	-	-	-
	W ₁ - X	h	-	-	-	-	10.17	12.00	-	-	-	-
	X - R	h	-	-	-	-	3.00	11.83	-	-	-	-
	P- W ₂	h	-	-	-	-	-	-	12.50	7.50	16.00	4.17
	W ₂ - A	h	-	-	-	-	-	-	12.67	x	18.50	7.17
	A	h	-	-	-	-	-	-	11.00	11.67	24.00	10.50
	A- W ₃	h	-	-	-	-	-	-	11.00	1.33	24.00	x
	W ₃ - R	h	-	-	-	-	-	-	-	-	22.33	x
	S _e	h	3.00	18.00	6.33	6.00	2.17	4.67	2.67	3.33	12.00	4.83
	T – Temperature		RH – Relative Humidity		HF – Density of heat flux rate							
P - One coat universal plaster		R - Lime-cement mortar		X - PIR insulation board								
W ₁ - Perforated brick layer		W ₂ - Solid brick layer		W ₃ - Frogged brick layer								
A - No ventilated air cavity		S _i – Surface interior		S _e – Surface exterior								

HIGHLIGHTS

- Laboratory scale thermal performance study of simple and double brick walls.
- Pervious mortar rendered walls in summer and winter scenarios were considered.
- Double (cavity) walls showed condensation in the non-ventilated air cavity.
- Rendering improved thermal performance but increased condensation risk.
- Effective retrofitting depends on materials, wall layouts and climate conditions.

Laboratory characterization of brick walls rendered with a pervious lime-cement mortar

I. Palomar ^{a,1}, G. Barluenga ^a, R.J. Ball ^b, M. Lawrence ^b

^a Department of Architecture, University of Alcalá, Spain

^b BRE Center for Innovative Construction Materials, Department of Architecture & Civil Engineering, University of Bath, UK

ABSTRACT

A laboratory study investigating important thermal retrofitting solutions for simple and double (cavity) brick walls is presented. Test walls were modified using materials of current interest including an external pervious lime-cement mortar render and insulation board prior to evaluation. Laboratory simulations of steady-state winter and summer scenarios were performed using apparatus comprising two opposing climate chambers. Temperature, relative humidity and heat flux rate were monitored with surface sensors every 10 minutes until stabilization on each wall type, retrofitting solution and climate scenario. The temperature and relative humidity profiles, heat flux, surface temperature difference, thermal conductance, condensation risk and stabilization times were assessed. Comparisons between simple and double (cavity) brick walls showed significant differences and a high condensation risk in the non-ventilated air cavity of the double wall. The pervious lime-cement mortar render enhanced substantially the thermal performance of the single wall although increased the condensation risk of the double (cavity) wall. As expected, the insulation layer reduced the thermal conductance of the wall, although the improvement in a summer scenario was considerably lower than in winter. The different performance observed between winter and summer steady-state conditions emphasized the importance of the heat and mass transfer coupling effect. Therefore, this work proves that effective retrofitting depends on materials, wall layouts and climate conditions. These experimental results provide essential knowledge about assessing the effects of common retrofitting solutions especially under hot-dry summer scenarios.

KEYWORDS

Brick walls; Pervious mortar; Retrofitting; Thermal performance; Heat and moisture transfer.

¹ Corresponding author. Departamento de Arquitectura. Escuela de Arquitectura, Universidad de Alcalá, C. Santa Úrsula, 8. Alcalá de Henares, 28801 Madrid, Spain. Tel.: +34 918839239; fax: +34 918839246 - *E-mail address*: irene.palomar@uah.es (I.Palomar)

1 Introduction

Existing dwelling buildings are part of a large building stock characterized by a large energy consumption, according to current energy efficiency standards [1, 2]. In the case of Spain, around 70% of the dwelling stock was built before the first national energy efficiency regulation was put into force in 1979, and 45% was built between 1960 and 1980 [3]. Due to its low energy efficiency, the residential sector is responsible for over 20% of the total energy consumption in Spain [4]. Thus, energy efficiency improvement has become a main concern and effective retrofitting techniques and materials are required.

Retrofitting this dwelling stock, which includes historical and traditional buildings, is a balance among reducing energy consumption, improving long-term building performance and satisfying today's functional requirements [5]. The most common (and cheapest) retrofitting solution for those buildings is an External Thermal Insulation Composite System (ETICS) [2]. However, some issues arise due to the embodied energy increase of traditional walls [6] and its low adaptability to specific insulation thickness and hygrothermal performance [7] that could produce moisture accumulations and organic growth in cold climates [8] and overheating in summertime [9]. On the other hand, façade retrofitting often requires the substitution of deteriorated traditional mortars, which becomes an opportunity to fulfill the nowadays building requirements through the design of new mortar coatings [10, 11, 12, 13]. Considering this, new pervious lime-cement mortars (PLCM) with short cellulose fibers (CF) have been designed to improve thermal and acoustic properties, fulfilling conservation, aesthetic, structural, service-life and construction issues [14, 15]. The main characteristic of PLCM is the lack of fine aggregate particles that creates an interconnected void network where spherical aggregate particles are surrounded by a shell of lime-cement paste and CF [16].

According to the literature [17], brick wall façades of those residential buildings can have one or two brick layers. Double walls were traditionally built with an intermediate non-ventilated air cavity. Due to the 70's energy crisis, a thermal insulation layer of 30-40 mm was typically incorporated between the brick layers, filling the air cavity. Before 1960, one layer brick walls were a common solution, using solid bricks, and lately 360 mm perforated bricks or even 120 mm hollow bricks.

As the new energy efficiency regulations come into force [1, 5], many brick wall facades were retrofitted with different types of renders, achieving various levels of effectiveness depending on the wall typology and climate scenario. Some studies reproduce common typologies and climate conditions, focusing on factors affecting thermal performance of lime or cement mortars, such as moisture content dependency [18, 19], the interface phenomena in a multiple layer wall [20] or the overestimation of traditional materials and wall properties, due to a lack of experimental data for computer models [21]. However, these results cannot be extrapolated to

121
122 other climate conditions as those characterized by high seasonal variations, large diurnal daily ranges and
123 high temperature and low relative humidity on summer days, which are typical of Southern Europe's climate
124 [22], since operating conditions affect the thermal performance of standard and retrofitted walls [6].
125

126
127 The hygrothermal performance of building materials and façade walls can be studied using mathematical and
128 computer models simulating the coupled effect of heat and moisture transfer through multilayer walls [23, 24,
129 25]. However, these algorithms require reliable material properties from laboratory characterization [26] or
130 involve a long-term monitoring to ensure reliability and overestimate pre-standard buildings performance [27].
131 Other alternative methods such as outdoor test cells or on-site assessment methods have been reported,
132 which allow consideration of dynamic boundary conditions [28, 29]. Laboratory simulation tests have also been
133 widely used, creating "artificial on-site conditions" with climatic chambers and reproducing either quasi steady-
134 state or dynamic scenarios [7, 30, 31, 32, 33]. Considering both the full-scale and laboratory tests, climate
135 scenarios can be easily applied to any wall layout in the laboratory-controlled conditions to estimate its
136 hygrothermal behavior [34]. Only few studies used a complete approach that included laboratory tests, outdoor
137 test cells, dynamic identification techniques, model calibration, simulation and full-scale building monitoring
138 [35].
139

140 This paper presents an experimental program aimed to investigate the effect of a pervious lime-cement mortar
141 render (PLCM) with and without an insulation board for thermal retrofitting of simple and double (cavity) brick
142 walls. Winter and summer steady-state scenarios were simulated using two climatic chambers applied on both
143 sides of the test walls with and without rendering. Temperature, relative humidity and heat flux were monitored.
144 The effectiveness of the retrofitting solution for each wall type, retrofitting solution and climate scenario was
145 assessed.
146
147
148

159 **2 Experimental program**

160
161 Two wall types, simple and double (cavity) brick walls, two retrofitting solutions including pervious lime-cement
162 mortars (PLCM) and two climate scenarios, steady state winter and summer, were experimentally
163 characterized. The walls and scenarios used in this study reproduce common constructive typologies and
164 climate conditions characterized by high seasonal variations and high temperature and low relative humidity
165 on summer. Two climate chambers were placed opposite one to another on each side of the testing wall to
166 simulate indoor and outdoor conditions. Temperature, relative humidity and heat flux sensors were used to
167 monitor hygrothermal parameters and the measurements were recorded every 10 minutes for at least 24 hours
168 after steady-state conditions were reached. Temperature (T) and relative humidity (RH) profiles, density of
169 heat flux rate (HF), surface temperature difference (ΔT), thermal conductance (Λ), condensation risk (CR) and
170
171
172
173
174
175
176
177
178
179
180

181
182 stabilization time (t_s) were analyzed. The experimental results were used to compare the different brick walls,
183
184 retrofitting solutions and climate scenarios.
185

186 2.1 Materials

187
188
189 The materials used in the study were:
190

- 191 • Three clay bricks (Category II, HD):
 - 192 ○ vertically perforated bricks (VPB) of 215 x 102.5 x 65 mm,
 - 193 ○ frogged bricks (FB) of 215 x 102.5 x 65 mm,
 - 194 ○ solid bricks (SB) of 215 x 102.5 x 35 mm.
 - 195
 - 196
 - 197
- 198 • Four binders:
 - 199 ○ an air lime class CL 90-S,
 - 200 ○ a white cement CEM I 52.5 R –SR5,
 - 201 ○ a cement type CEM II/B-V/32.5R,
 - 202 ○ a one coat gypsum plaster class B4/20/2.
 - 203
 - 204
 - 205
 - 206
- 207 • Two aggregates: a siliceous sand (0-4 mm) and a gap-graded limestone sand (2-3 mm).
- 208
- 209 • Short cellulose fibers of length 1 mm - Fibracel® BC-1000 ($\varnothing 20\mu\text{m}$) - supplied by Omya Clariana S.L.
- 210
- 211 • Rigid insulation board of polyisocyanurate foam and low emissivity foil facings (X) of 50 mm.

212
213 The binder materials were used to produce a retrofitting render (R), a Plaster (P) and a Joint mortar (J),
214 prepared as follows:
215

- 216 • Retrofitting render (R): Pervious lime-cement mortar (PLCM) with gap-graded limestone sand (1:1:6
217 by volume lime/cement/sand ratios), cellulose fibres (1.5% of the total dried mortar's volume) and 0.94
218 water to binder ratio (w/b). This mixture was selected out of twelve evaluated in a previous study due
219 to the particular suitability for external rendering when considering the technical, functional and
220 performance requirements [14]. The use of cellulose fibers in PLCM improved the thermal and acoustic
221 performance - the lowest thermal conductivity coefficient and the highest noise reduction was
222 observed from a previous study as both paste thickness and active void size were modified [16].
223
- 224 • Plaster (P): A one coat gypsum plaster with w/b = 0.45
225
- 226 • Joint mortar (J): Cement mortar with continuous siliceous sand (1:6 by volume) and w/b = 1
227
228
229
230
231

232 Table 1 summarizes some materials' properties as bulk density (ρ), moisture-dependent water vapor diffusion
233 resistance factor (μ), thermal conductivity (λ), specific heat (c_p) and thermal diffusivity (α). Thermal diffusivity
234 (α) was calculating according to Eq. (1) [36]:
235
236
237

$$\alpha = \frac{\lambda}{\rho \cdot c_p} \quad (1)$$

where λ is the thermal conductivity of the material, ρ is bulk density and c_p specific heat.

The retrofitting render (R) was previously characterized and showed a suitable thermal and acoustic performance [14, 15, 16]. The gypsum plaster thermo-physical properties were experimentally characterized. Nominal properties for bricks [37] and insulation board provided by the manufacturers were considered, although slight differences can be expected due to the effect of temperature, moisture and aging [38].

2.2 Façade brick wall layouts

Five wall configurations, three single walls and two double (cavity) walls, were fabricated. Fig. 1 shows the 450 x 440 mm brick wall cross-sections.

The reference single wall (REF(S)) was built with one 103 mm thick layer of vertically perforated bricks (VPB) and a joint cement mortar (J), while the reference double (cavity) wall (REF(D)) was built with two layers, 35 mm solid bricks (SB) and 103 mm frogged bricks (FB), with a 40 mm non-ventilated air cavity (A) in between.

The interior side of both walls was coated with 15 mm gypsum plaster (P).

Then, the external side of both walls was rendered with a 25 mm pervious lime-cement mortar (R), named REF(S)+R and REF(D)+R respectively. The single wall was also retrofitted combining a 50 mm thick thermal insulation board (X) with the pervious lime-cement render (R), noted as REF(S)+X+R. A polyisocyanurate (PIR) insulation panel was selected to reduce insulation thickness while complying with energy efficiency standards [39, 40]. Besides, PIR has the best fire resistance among foam plastics [39].

The design thermal conductance (Λ_c) of the wall layouts was calculated according to Eq. (2) [36]:

$$\Lambda_c = \frac{1}{\sum_j \frac{d_j}{\lambda_j}} \quad (2)$$

where λ is the thermal conductivity and d is the thickness of each layer (j) in Table 1.

2.3 Experimental methods

Fig. 2 shows the experimental setup designed for this study. The walls were built inside a plywood framework, sealed and thermally isolated with polyisocyanurate foam to allow a one-dimensional heat and moisture flux. Samples were stored under laboratory conditions at $22 \pm 2^\circ\text{C}$ and $60 \pm 10\%$ RH until testing. The framework with the wall was then placed between two climate chambers simulating the effect of different climate conditions on the walls. Temperature (T) and relative humidity (RH) were set using two TAS MTCL-135 climate

301 chambers with HMI Control Systems which was used to produce heat and moisture flux that simulated winter
302 and summer scenarios. The water vapor density (v) for each scenario was estimated according to ISO 13788
303 [40]. The interior conditions were set at 23°C and 50 ±5% RH ($v = 0.0103 \pm 0.001 \text{ kg/m}^3$) and the exterior
304 conditions were 12°C, 80±5% RH ($v = 0.0085 \pm 0.0005 \text{ kg/m}^3$) for winter and 31°C, 40±5% RH ($v = 0.0128 \pm$
305 0.002 kg/m^3) for summer. These conditions were selected to simulate climates with high seasonal variations
306 and high temperature and low RH in summer.
307

308 K type thermocouples and relative humidity sensors (HIH4000) were used to monitor the interior of the
309 chambers and the surfaces of all the layers of the walls at 10 minute intervals. A heat flux sensor (HFP01 by
310 Hukseflux) was placed in the interior side of the walls. The operational error in the heat flux meter (HFM) was
311 calculated as 10% to 22%, according to ISO 9869 [42]. Temperature (T), relative humidity (RH) and density of
312 heat flux rate (HF) were monitored on the walls and the results were analyzed after a steady-state regime was
313 reached. Afterwards, laboratory-experimental thermal conductance (Λ), risk of surface and interstitial
314 condensation (CR) and transition time (t_s) were calculated and used to compare single and double walls with
315 and without retrofitting solutions in winter and summer scenarios. Laboratory-experimental thermal
316 conductance (Λ) of the wall layouts was estimated using the ratio between the mean density of heat flow rate
317 (HF) and mean temperature difference between the interior ($T_{s,i}$) and exterior ($T_{s,e}$) surfaces after a steady-
318 state regime was reached over a long enough period of time [41,42].
319

333 **3 Experimental results**

334 Two wall types, simple and double cavity brick walls, two retrofitting solutions with an exterior pervious lime-
335 cement mortar render with and without an insulation board, and two steady-state climate scenarios, winter and
336 summer, were experimentally characterized.
337

342 **3.1 Laboratory characterization of simple brick walls**

343 Temperature (T) and relative humidity (RH) cross-sections of the single walls in steady-state winter and
344 summer scenarios are plotted in Fig. 3. It can be observed that the addition of exterior pervious lime-cement
345 mortar render and an insulation board produced different effects.
346

347 In the winter scenario, the temperature difference (ΔT) for the brick layer (W_1) was 6.45 °C in the reference
348 single wall REF(S), whereas ΔT were 3.95 and 0.52 °C for rendered (REF(S)+R) and insulated (REF(S)+X+R)
349 single walls respectively. The highest RH values were found on the exterior pervious lime-cement mortar
350

361 render (R) both in REF(S)+R and REF(S)+X+R walls. However, RH was lower than 100% and there was no
362 surface or interstitial condensation in any single wall in the winter scenario.
363
364

365 In the summer scenario, the addition of exterior pervious lime-cement mortar render (R) reduced the
366 temperature difference of the brick layer (W_1) from 4.20 °C to 2.47 °C. In addition, the interior plaster (P) also
367 showed lower temperatures. When an insulation board (X) was added, its temperature difference was 5.68 °C
368 and almost zero in the other layers. RH cross-sections showed similar values for both REF(S) and REF(S)+R.
369 On the other hand, the addition of an insulation board (X) increased RH between W_1 and X layers, although
370 no surface or interstitial condensation was recorded.
371
372
373
374
375

376 **3.2. Laboratory characterization of double (cavity) brick walls**

377
378 Fig. 4 shows temperature (T) and relative humidity (RH) cross-sections of the double (cavity) walls measured
379 in steady-state winter and summer scenarios, showing the effect of a non-ventilated air cavity (REF(D)) and
380 an exterior pervious lime-cement mortar render (REF(D)+R).
381
382
383
384

385 REF(D) temperature cross-section in the winter steady-state scenario showed that the interior brick layer (W_2),
386 the non-ventilated air cavity (A) and the exterior brick layer (W_3) had temperature differences (ΔT) of 1.39, 4.21
387 and 3.53 °C, respectively. In the case of REF (D)+R, the render (R) showed a ΔT of 2.26 °C and halved the
388 temperature difference of the non-ventilated air cavity to 2.20 °C. The brick layers (W_2 and W_3) and plaster (P)
389 had similar temperatures in both walls. The RH cross-section of REF(D) showed a high relative humidity in the
390 air cavity (A) and interstitial condensation occurred. Nevertheless, no surface condensation in winter conditions
391 was recorded. The same happened on the rendered wall, REF(D)+R: interstitial condensation occurred,
392 especially in the exterior brick layer (W_3), but no surface condensation was recorded.
393
394
395
396
397
398

399 In the summer scenario, the interior brick layer (W_2), the non-ventilated air cavity (A) and the exterior brick
400 layer (W_3) had a temperature differences (ΔT) of 1.95, 1.54 and 4.38 °C, respectively. Therefore, the non-
401 ventilated air cavity (A) had less effect on temperature cross-section in summer than in winter, whereas the
402 external brick layer (W_3) showed the higher thermal difference. The addition of exterior PLCM render (R)
403 reduced the temperature difference of the interior brick layer (W_2) and the non-ventilated air cavity (A) to one
404 half and the external brick layer (W_3) to one third which was the lowest recorded in this layer. The render layer
405 had a ΔT of 3.55 °C, which corresponded to 44% of the total temperature difference while in the winter scenario
406 a temperature difference of only 22% was reached. Therefore, the rendering produced a larger improvement
407 on double walls in summer than in winter. RH of REF(D) was also different in summer than in the winter
408 scenario, as the brick layer (W_3) condensed water in summer. Moreover, the addition of the rendering
409 (REF(D)+R) extended the area affected by interstitial condensation to the air cavity (A) and the external brick
410
411
412
413
414
415
416
417
418
419
420

421 layer (W_3). However, this cannot be considered a problem because the condensed water can easily evaporate
422 in summer conditions.
423
424

425 **4 Analysis and discussion**

426
427
428
429 The laboratory data was used to compare the different brick walls, retrofitting solutions and scenarios. Density
430 of heat flux rate (HF), surface temperature difference (ΔT), thermal conductance (Λ), stabilization time ($t_{s, HF}$;
431 $t_{s, \Delta T}$) and condensation risk (CR) during steady-state winter and summer conditions were analyzed and the
432 experimental results summarized in Table 2. One-dimensional heat and moisture flux through the walls can
433 be assumed for both steady-state scenarios. In winter, the heat and moisture transfer occurred from the inside
434 to the outside (outwards), while in summer, the flux was from the outside to the inside (inwards).
435
436
437
438
439
440

441 **4.1 Effect of the non-ventilated air cavity on the wall performance**

442
443
444 Table 2 shows the laboratory measurements of density of heat flux rate (HF) and surface temperature
445 difference (ΔT) of single and double walls. It can be observed that the ΔT value reached an asymptotic situation
446 earlier than HF ($t_{s, \Delta T} < t_{s, HF}$). The larger difference in double walls can be partially attributed to the water
447 condensed in the non-ventilated air cavity (Fig. 4). HF stabilization occurred after the moisture flow ended, due
448 to the heat and mass transfer coupling effect.
449
450
451

452
453 The effect of the non-ventilated air cavity on the wall performance can be evaluated comparing the heat flux
454 (HF), surface temperature difference (ΔT), thermal conductance (Λ), stabilization time ($t_{s, \Delta T}$; $t_{s, HF}$) and
455 condensation risk (CR) during steady-state winter and summer conditions (Table 2). Double brick walls
456 reduced the heat flux of single walls in both scenarios by almost three times. This can be explained by the low
457 thermal conductivity of the still air in the non-ventilated air cavity (A). In addition, the surface temperature
458 difference was around 1°C higher in the double compared to the simple wall. Although the non-ventilated air
459 cavity (A) reduced significantly the thermal conductance, a high condensation risk was observed in all
460 scenarios and the air cavity would require drainage. Concerning the stabilization time of HF, REF(D) doubled
461 the time of REF(S) to stabilize in winter, whereas both walls stabilized almost simultaneously in summer. The
462 differences of $t_{s, HF}$ can be attributed to the condensed water and moist air in the non-ventilated air cavity in
463 winter and summer which would modify the materials' specific heat and thermal conductivity, increasing heat
464 storage [43].
465
466
467
468
469
470
471
472
473
474
475
476
477
478
479
480

4.2 Assessment of the retrofitting solutions

In this section, the effect of a pervious lime-cement mortar render (R) and an insulation board (X) on single and double brick walls was evaluated.

4.2.1 Effect of pervious lime-cement mortar render (R)

Rendering the simple and double brick walls with a pervious lime-cement mortar produced two effects related to the heat and moisture transfer. On one hand, the insulation capacity of the mortar reduced the measured thermal conductance (Λ) (Table 2). This reduction was larger in the simple wall compared to the double wall and also in the summer conditions compared to the winter conditions. In addition, the rendered double wall REF(D)+R showed a similar thermal conductance as the insulated single wall REF(S)+X+R in the summer scenario.

The second effect was related to the low vapor permeability of the mortar which modified moisture transfer. The consequences on double brick walls can be summarized as an increase of condensation inside the non-ventilated air cavity and an extension of the layers affected by interstitial condensation risk (Fig.4).

The combined effect of the render on the heat and moisture transfer also delayed the heat flux stabilization time ($t_{s,HF}$) in all scenarios and wall types, except for the double wall in winter conditions. REF(D)+R in summer conditions showed the highest heat flux stabilization time. The explanation can be found on its insulation capacity and low permeability jointly with its thermal inertia, as the moisture content modified specific heat and increased heat storage of building materials [43].

Accordingly, the incorporation of the render layer on the external side of the walls produced a reduction of the energy needed to keep the interior conditions which would mean lower energy consumption for air conditioning. It would also reduce the thermal variations of the brick layers which would improve their dimensional stability, reducing the cracking risk of the wall under severe climate variations and would improve wall durability [9]. However, the thermal difference between render and brick wall would require a good adherence between the mortar and the brick layer.

4.2.2 Effect of the insulation board (X)

The incorporation of a thermal insulation board, jointly with the mortar render, on the exterior side of the single wall as an improved retrofitting solution produced a significant reduction of heat flux (Table 2), as expected [44]. However, the overall improvement depended on the climate conditions: the thermal conductance measured (Table 2) in the winter scenario was half of the design value (Fig. 1), remarkably better than

541 expected, while in the summer scenario the value was doubled. Therefore, the effect of the insulation board
542 was strongly reduced in summer conditions. Those results agree with the literature: differences between
543 experimental and design values when insulation was included [21] and those differences are larger in summer
544 conditions than in winter [39].

545 A secondary effect of the insulation board was the vapor barrier effect due to its extremely low vapor
546 permeability. This property significantly reduced heat flux stabilization time, especially in winter scenario,
547 reaching a value similar to the rendered double wall (REF(D)+ R) in winter which was highly affected by
548 condensation. This can be related to the reduction of vapor transfer jointly with the flux and moisture direction
549 in each case (outwards in winter and inwards in summer), and it could lead to an increased risk of damage in
550 the render layer in winter and the plaster in summer due to moisture accumulation and of interfacial
551 mechanisms [20].

562 **4.3 Temperature (T), relative humidity (RH) and heat flux (HF) stabilization time**

563 Stabilization began in the external layers and was reached later in the internal layers, both in winter and
564 summer scenarios, except for the non-ventilated air cavity due to its lack of thermal inertia. It was observed
565 that the time to reach a steady-state regime depends on the wall type, retrofitting solutions and climate scenario
566 (Table 2 and 3). The single brick walls took at least 18 hours to stabilize RH in summer scenario. On the other
567 hand, only REF(S)+X+R showed a similar behaviour (14 hours) in winter. T values, which stabilized the last in
568 the case of double cavity brick walls, required at least 12 hours in all the climate scenarios.

569 In general, single walls stabilized slightly faster in winter than in summer. When the three single wall layouts
570 were compared (Table 3), REF(S)+X+R exhibited the lower stabilization time of HF, followed by REF(S) and
571 REF(S)+R. Consequently, REF(S)+X+R took less time to reach an equilibrium compared to other single walls.
572 In double walls (Table 3), REF(D)+R showed the longest stabilization time in summer for both T and HF, but
573 not for RH. However, this wall was the fastest to stabilize HF in winter, with stabilization times shorter than
574 those obtained for single walls.

575 Regarding the three parameters evaluated, RH stabilized before T and HF, with the exception of REF(S) in
576 summer and the thermally insulated single wall in both scenarios, REF(S)+X+R, which showed the opposite.
577 In this case (REF(S)+X+R), the delay on RH values in Table 3 corresponded to insulation-render interlayer (X-
578 R) in winter and to plaster-internal brick interlayer (P -W₁) in summer. As far as there were peaks on RH and
579 not on temperature stabilization time data (Table 3), it can be assumed that this change was due to the vapor
580 barrier effect of the insulation board. In double walls, HF always stabilized before T. The heat and mass transfer
581 coupling effect can explain why heat flow stabilization occurred after the moisture flow ended.

4.4 Effective brick wall retrofitting in different climate scenarios

The experimental results pointed out that the simple and double brick walls and retrofitting solutions behaved different in winter and summer scenarios, which agrees with previous studies [45]. Thermal conductance measured in the laboratory tended to be higher in winter than in the summer scenario and different from the design values. Heat flux stabilization time was longer in summer than in winter scenario. The effect of climate conditions also depended on the layers affected by interstitial condensation in double brick walls, due to a heat and moisture transfer coupling effect which would modify the materials' specific heat, thermal conductivity and heat storage capacity [43]. It would be a positive effect in summer (inwards heat and moisture transfer) due to the increase of thermal capacity, but a negative effect in winter (outwards transfer) due to the increase of thermal conductivity.

The use of an external insulation board on simple brick walls reduced the heating demand significantly in winter. However, the insulation capacity depended on the climate conditions and was strongly reduced in summer, as reported previously [39]. On the other hand, the use of the pervious lime-cement mortar render on the external side of the double brick walls produced a reduction of the cooling energy needed to maintain the interior conditions in summer which would mean less energy consumption in air conditioning [47, 34]. Therefore, the effectiveness of a retrofitting solution depends on both the material properties and the climate conditions.

Consequently, heating and cooling demand would be underestimated if the heat and moisture coupling effect is not considered. This is in agreement with other authors who highlighted the need of different strategies than thermal insulation to enhance the thermal performance of buildings in climates with a hot summer [46].

5 Conclusions

This paper presents a laboratory characterization of two wall types, simple and double (cavity) brick walls, two retrofitting solutions, a pervious lime-cement mortar render with and without an insulation board, and two climate scenarios, steady state winter and summer simulated using two climate chambers. The experimental program measured temperature, relative humidity (RH) and heat flux rate (HF). Laboratory-experimental thermal conductance, surface and interstitial condensation and temperature, RH and heat flux stabilization time were calculated. The main findings of the study are:

- The measured results of experimental thermal conductance were different from the calculated values and depended on the climate conditions.

- 661
662
663
664
665
666
667
668
669
670
671
672
673
674
675
676
677
678
679
680
681
682
683
684
685
686
687
688
689
- The hygrothermal stabilization of the wall occurred first on the outer layers and afterwards in the inner layers. RH stabilized first, then temperature and HF stabilized the last, due to the heat and moisture coupling effect.
 - Double (cavity) brick walls showed better thermal performance than simple walls due to the non-ventilated air cavity. However, double brick walls showed a high condensation risk in both winter and summer scenarios and the air cavity would require drainage.
 - The use of an exterior pervious lime-cement mortar render (R) improved the thermal performance of both single and double walls, delaying the heat flux stabilization time. Although, it can increase interstitial condensation in double walls due to the render's low vapor permeability.
 - The use of an external insulation board (X) improved the thermal performance in winter conditions, significantly reducing the heat flux and, therefore, the energy required for heating. However, the behavior in summer scenario was significantly worse than expected.
 - The differences between expected and measured results can be attributed to the effect of moisture transfer on heat transfer and wall thermal properties. Therefore, the effectiveness of a retrofitting solution depends on both the material properties, and the climate conditions.

690 **Acknowledgments**

691
692
693
694
695
696
697
698
699

The authors wish to acknowledge the help of Dr Eshrar Latif and Dr Daniel Maskell, and the contribution on the testing preparation of the technical staff of the Engineering & Design Technical Services at the Department of Architecture and Civil Engineering, University of Bath. Some of the components were supplied by Omya Clariana S.L.

700 **Funding**

701
702
703
704
705

Financial support for this research was provided by the Trainee Research Personnel Mobility Grant (Movilidad PIF-UAH 2015) and Grant for training of Lecturers (FPU-UAH 2013), funded by the University of Alcala.

706 **Declarations of interest**

707
708
709
710
711
712
713
714
715
716
717
718
719
720

None

References

- [1] Directive 2010/31/EU of the European Parliament and of the Council of 19 May 2010 on the energy performance of buildings. Official Journal of the European Union, n° L 153, of 18 June 2010
- [2] Ma Z, Cooper P, Daly D, Ledo L (2012) Existing building retrofits: Methodology and state-of-the-art. Energy Build 55: 889-902. <https://doi.org/10.1016/j.enbuild.2012.08.018>
- [3] "Owner-occupied dwellings by type and year of construction of the building" (2001) Eurostat database, European Commission, Luxembourg. http://ec.europa.eu/eurostat/web/products-datasets/product?code=cens_01ndpercons. Accessed 10 May 2016
- [4] Pérez-Lombard L, Ortiz J, Pout C (2008) A review on buildings energy consumption information. Energy Build 40(3):394-398. <https://doi.org/10.1016/j.enbuild.2007.03.007>
- [5] Webb AL (2017) Energy retrofits in historic and traditional buildings: A review of problems and methods. Renewable Sustainable Energy Rev 77:748-759. <https://doi.org/10.1016/j.rser.2017.01.145>
- [6] Kyriakidis A, Michael A, Illampas R, Charnpis DC, Ioannou I (2018) Thermal performance and embodied energy of standard and retrofitted wall systems encountered in Southern Europe, Energy 161: 1016-1027. <https://doi.org/10.1016/j.energy.2018.07.124>.
- [7] Johansson P, Geving S, Hagentoft CE, Jelle BP, Rognvik E, Kalagasidis AS, Time B (2014) Interior insulation retrofit of a historical brick wall using vacuum insulation panels: Hygrothermal numerical simulations and laboratory investigations. Build Environ 79:31-45. <https://doi.org/10.1016/j.buildenv.2014.04.014>
- [8] Künzle HM (1998) Effect of interior and exterior insulation on the hygrothermal behaviour of exposed walls. Mater Struct 31(2):99 -103
- [9] Gupta R, Gregg M (2018) Assessing energy use and overheating risk in net zero energy dwellings in UK. Energy Build 158:897-905. <https://doi.org/10.1016/j.enbuild.2017.10.061>
- [10] Govaerts Y, Hayen R, de Bouw M, Verdonck A, Meulebroeck W, Mertens S, Grégoire Y (2018) Performance of a lime-based insulating render for heritage buildings. Constr Build Mater 159:376-389. <https://doi.org/10.1016/j.conbuildmat.2017.10.115>
- [11] Bianco L, Serra V, Fantucci S, Dutto M, Massolino M, (2015) Thermal insulating plaster as a solution for refurbishing historic building envelopes: First experimental results. Energy Build 95:86-91. <https://doi.org/10.1016/j.enbuild.2014.11.016>
- [12] Ibrahim M, Biwole PH, Wurtz E, Achard P (2014) A study on the thermal performance of exterior walls covered with a recently patented silica-aerogel-based insulating coating. Build Environ 81:112-122. <https://doi.org/10.1016/j.buildenv.2014.06.017>

- 781
782
783
784
785
786
787
788
789
790
791
792
793
794
795
796
797
798
799
800
801
802
803
804
805
806
807
808
809
810
811
812
813
814
815
816
817
818
819
820
821
822
823
824
825
826
827
828
829
830
831
832
833
834
835
836
837
838
839
840
- [13] Stefanidou M (2014) Cement-based renders with insulating properties. *Constr Build Mater* 65: 427-431. <https://doi.org/10.1016/j.conbuildmat.2014.04.062>
- [14] Palomar I, Barluenga G, Puentes J (2015) Lime–cement mortars for coating with improved thermal and acoustic performance. *Constr Build Mater* 75: 306-314. <https://doi.org/10.1016/j.conbuildmat.2014.11.012>
- [15] Palomar I, Barluenga G (2017) Assessment of lime-cement mortar microstructure and properties by P- and S- ultrasonic waves. *Constr Build Mater* 139:334-341. <https://doi.org/10.1016/j.conbuildmat.2017.02.083>
- [16] Palomar I, Barluenga G (2018) A multiscale model for pervious lime-cement mortar with perlite and cellulose fibers. *Constr Build Mater* 160:136-144. <https://doi.org/10.1016/j.conbuildmat.2017.11.032>
- [17] Terés-Zubiaga J, Martín K, Erkoreka A, Sala JM (2013) Field assessment of thermal behaviour of social housing apartments in Bilbao, Northern Spain. *Energy Build* 67:118-135. <https://doi.org/10.1016/j.enbuild.2013.07.061>
- [18] Pavlík Z, Vejmelková E, Fiala L, Černý R (2009) Effect of moisture on thermal conductivity of lime-based composites. *Int J Thermophys* 30 (6):1999-2014. <https://doi.org/10.1007/s10765-009-0650-y>
- [19] Khan MI (2002) Factors affecting the thermal properties of concrete and applicability of its prediction models. *Build Environ* 37(6): 607-614. [https://doi.org/10.1016/S0360-1323\(01\)00061-0](https://doi.org/10.1016/S0360-1323(01)00061-0)
- [20] De Freitas VP, Abrantes V, Crausse P (1996) Moisture migration in building walls—Analysis of the interface phenomena. *Build Environ* 31(2):99-108. [https://doi.org/10.1016/0360-1323\(95\)00027-5](https://doi.org/10.1016/0360-1323(95)00027-5)
- [21] Walker R, Pavía S (2015) Thermal performance of a selection of insulation materials suitable for historic buildings. *Build Environ* 94(Part 1):155-165. <https://doi.org/10.1016/j.buildenv.2015.07.033>
- [22] Stazi F, Bonfigli C, Tomassoni E, Di Perna C, Munafò P (2015) The effect of high thermal insulation on high thermal mass: Is the dynamic behaviour of traditional envelopes in Mediterranean climates still possible? *Energy Build* 88:367-383. <https://doi.org/10.1016/j.enbuild.2014.11.056>
- [23] Qin M, Belarbi R, Ait-Mokhtar A, Nilsson LO (2009) Coupled heat and moisture transfer in multi-layer building materials. *Constr Build Mater* 23(2): 967-975. <https://doi.org/10.1016/j.conbuildmat.2008.05.015>
- [24] Skujans J, Vulans A, Iljins U, Aboltins A (2007) Measurements of heat transfer of multi-layered wall construction with foam gypsum. *Appl Therm Eng* 27(7):1219-1224. <https://doi.org/10.1016/j.applthermaleng.2006.02.047>
- [25] Bellia L, Minichiello F (2003) A simple evaluator of building envelope moisture condensation according to an European Standard. *Build Environ* 38(3): 457-468. [https://doi.org/10.1016/S0360-1323\(02\)00060-4](https://doi.org/10.1016/S0360-1323(02)00060-4)

- 841
842 [26] López O, Torres I, Guimarães AS, Delgado JMPQ, de Freitas VP (2017) Inter-laboratory variability
843 results of porous building materials hygrothermal properties. *Constr Build Mater* 156:412-423.
844 <https://doi.org/10.1016/j.conbuildmat.2017.08.184>
845
846
847 [27] Lucchi E (2017) Thermal transmittance of historical brick masonries: a comparison among standard
848 data, analytical calculation procedures, and in situ heat flow meter measurements. *Energy Build* 134:171-184.
849 <https://doi.org/10.1016/j.enbuild.2016.10.045>
850
851
852 [28] Jiménez MJ, Porcar B, Heras MR (2009) Application of different dynamic analysis approaches to the
853 estimation of the building component U value. *Build Environ* 44(2):361-367.
854 <https://doi.org/10.1016/j.buildenv.2008.03.010>
855
856
857 [29] Toman J, Vimrová A, Černý R (2009) Long-term on-site assessment of hygrothermal performance
858 of interior thermal insulation system without water vapor barrier. *Energy Build* 41(1):51-55.
859 <https://doi.org/10.1016/j.enbuild.2008.07.007>
860
861
862 [30] Latif E, Tucker S, Ciupala MA, Wijeyesekera DC, Newport DJ, Pruteanu M (2016) Quasi steady state
863 and dynamic hygrothermal performance of fibrous Hemp and Stone Wool insulations: Two innovative
864 laboratory based investigations. *Build Environ* 95:391-404. <https://doi.org/10.1016/j.buildenv.2015.10.006>
865
866
867 [31] Pavlík Z, Černý R (2008) Experimental assessment of hygrothermal performance of an interior thermal
868 insulation system using a laboratory technique simulating on-site conditions. *Energy Build* 40(5): 673-678.
869 <https://doi.org/10.1016/j.enbuild.2007.04.019>
870
871
872 [32] Moradas PA, Silva PD, Castro-Gomes JP, Salazar MV, Pires L (2012) Experimental study on
873 hygrothermal behaviour of retrofit solutions applied to old building walls. *Constr Build Mater* 35:864-873.
874 <https://doi.org/10.1016/j.conbuildmat.2012.04.138>
875
876
877 [33] Palumbo M, Lacasta AM, Giraldo MP, Haurie L, Correal E (2018) Bio-based insulation materials and
878 their hygrothermal performance in a building envelope system (ETICS). *Energy Build* 174:147-155.
879 <https://doi.org/10.1016/j.enbuild.2018.06.042>
880
881
882 [34] Ferrari S, Zanotto V (2013) The thermal performance of walls under actual service conditions:
883 Evaluating the results of climatic chamber tests. *Constr Build Mater* 43: 309-316.
884 <https://doi.org/10.1016/j.conbuildmat.2013.02.056>
885
886
887 [35] Strachan PA, Vandaele L (2008) Case studies of outdoor testing and analysis of building components.
888 *Build Environ* 43(2):129-142. <https://doi.org/10.1016/j.buildenv.2006.10.043>
889
890
891 [36] UNE-EN ISO 7345 (1996) Thermal insulation. Psychical quantities and definitions. Spanish
892 Organization for Standardization (AENOR)
893
894
895
896
897
898
899
900

- 901
902 [37] UNE-EN 1745 (2013) Masonry and masonry products - Methods for determining thermal properties.
903 Spanish Organization for Standardization (AENOR)
904
905 [38] UNE-EN ISO 10456 (2007) Buildings materials and products. Hygrothermal properties. Tabulated
906 design values and procedures for determining declared and design thermal values. Spanish Organization for
907 Standardization (AENOR)
908
909 [39] Schiavoni S, D'Alessandro F, Bianchi F, Asdrubali F (2016) Insulation materials for the building sector:
910 A review and comparative analysis. Renewable Sustainable Energy Rev 62:988-1011.
911 <https://doi.org/10.1016/j.rser.2016.05.045>
912
913 [40] Pescari S, Tudor D, Tölgyi S, Maduta C (2015) Study concerning the thermal insulation panels with
914 double-side anti-condensation foil on the exterior and polyurethane foam or polyisocyanurate on the interior.
915 Key Eng. Mater 660, 2015: 244–248. <https://doi:10.4028/www.scientific.net/KEM.660.244>
916
917 [41] UNE-EN ISO 13788 (2001) Hygrothermal performance of buildings components and buildings
918 elements. Internal surface temperature to avoid critical surface humidity and interstitial condensation.
919 Calculation method. Spanish Organization for Standardization (AENOR)
920
921 [42] BS ISO 9869-1 (2014) Thermal insulation — Building elements — In-situ measurement of thermal
922 resistance and thermal transmittance. Part 1: Heat flow meter method. British Standards Institution (BSI)
923
924 [43] Jerman M, Černý R (2012) Effect of moisture content on heat and moisture transport and storage
925 properties of thermal insulation materials. Energy Build 53: 39-46.
926 <https://doi.org/10.1016/j.enbuild.2012.07.002>
927
928 [44] Cabeza LF, Castell A, Medrano M, Martorell I, Pérez G, Fernández I (2010) Experimental study on the
929 performance of insulation materials in Mediterranean construction. Energy Build 42(5):630-636.
930 <https://doi.org/10.1016/j.enbuild.2009.10.033>
931
932 [45] Mazzeo D, Oliveti G, Arcuri N (2016) Influence of internal and external boundary conditions on the
933 decrement factor and time lag heat flux of building walls in steady periodic regime. Appl Energy 164: 509-531.
934 <https://doi.org/10.1016/j.apenergy.2015.11.076>
935
936 [46] Corrado V, Paduos S (2016) New equivalent parameters for thermal characterization of opaque
937 building envelope components under dynamic conditions. Appl Energy 163:313-322.
938 <https://doi.org/10.1016/j.apenergy.2015.10.123>
939
940 [47] Aste N, Leonforte F, Manfren M, Mazzon M, (2015) Thermal inertia and energy efficiency – Parametric
941 simulation assessment on a calibrated case study. Appl Energy 145:111-123.
942 <https://doi.org/10.1016/j.apenergy.2015.01.084>
943
944
945
946
947
948
949
950
951
952
953
954
955
956
957
958
959
960

961
962
963
964
965
966
967
968
969
970
971
972
973
974
975
976
977
978
979
980
981
982
983
984
985
986
987
988
989
990
991
992
993
994
995
996
997
998
999
1000
1001
1002
1003
1004
1005
1006
1007
1008
1009
1010
1011
1012
1013
1014
1015
1016
1017
1018
1019
1020

List of figures and tables

Fig. 1 Vertical cross section of wall layouts (Λ_c = designed thermal conductance)

Fig. 2 Experimental setup for climate scenarios simulated using two climate chambers (distance in mm)

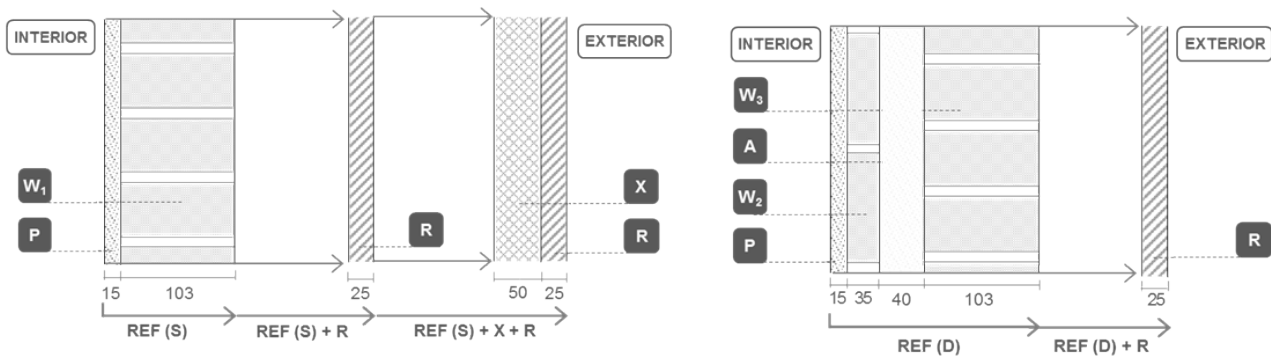
Fig. 3 Temperature and relative humidity steady-state winter and summer scenarios

Fig. 4 Temperature and relative humidity cross-sections of double (cavity) walls in steady-state winter and summer scenarios

Table 1 Materials' Properties

Table 2 Laboratory measured thermal parameters in winter and summer scenarios

Table 3 Temperature, relative humidity and heat flux stabilization time of single and double walls in winter and summer scenarios



Single Walls	Λ_c	Double Walls	Λ_c
REF (S)	4.99 W/m ² K	REF (D)	2.10 W/m ² K
REF (S) + R	3.03 W/m ² K	REF (D) + R	1.65 W/m ² K
REF (S) + X + R	0.38 W/m ² K		

A: No ventilated air cavity **R:** Lime-cement mortar **W₁:** Perforated brick layer **W₃:** Frogged brick layer
P: One coat universal plaster **X:** PIR insulation board **W₂:** Solid brick layer **Distances in mm**

Fig. 1 Vertical cross section of wall layouts (Λ_c = designed thermal conductance)

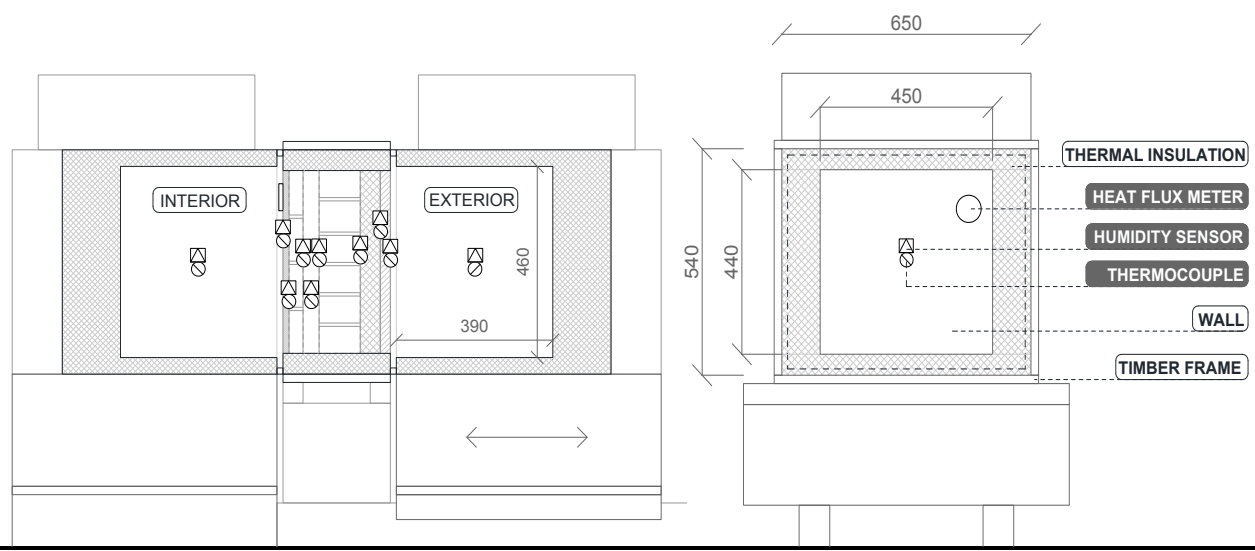


Fig. 2 Experimental setup for climate scenarios simulated using two climate chambers (distance in mm)

1081
 1082
 1083
 1084
 1085
 1086
 1087
 1088
 1089
 1090
 1091
 1092
 1093
 1094
 1095
 1096
 1097
 1098
 1099
 1100
 1101
 1102
 1103
 1104
 1105
 1106
 1107
 1108
 1109
 1110
 1111
 1112
 1113
 1114
 1115
 1116
 1117
 1118
 1119
 1120
 1121
 1122
 1123
 1124
 1125
 1126
 1127
 1128
 1129
 1130
 1131
 1132
 1133
 1134
 1135
 1136
 1137
 1138
 1139
 1140

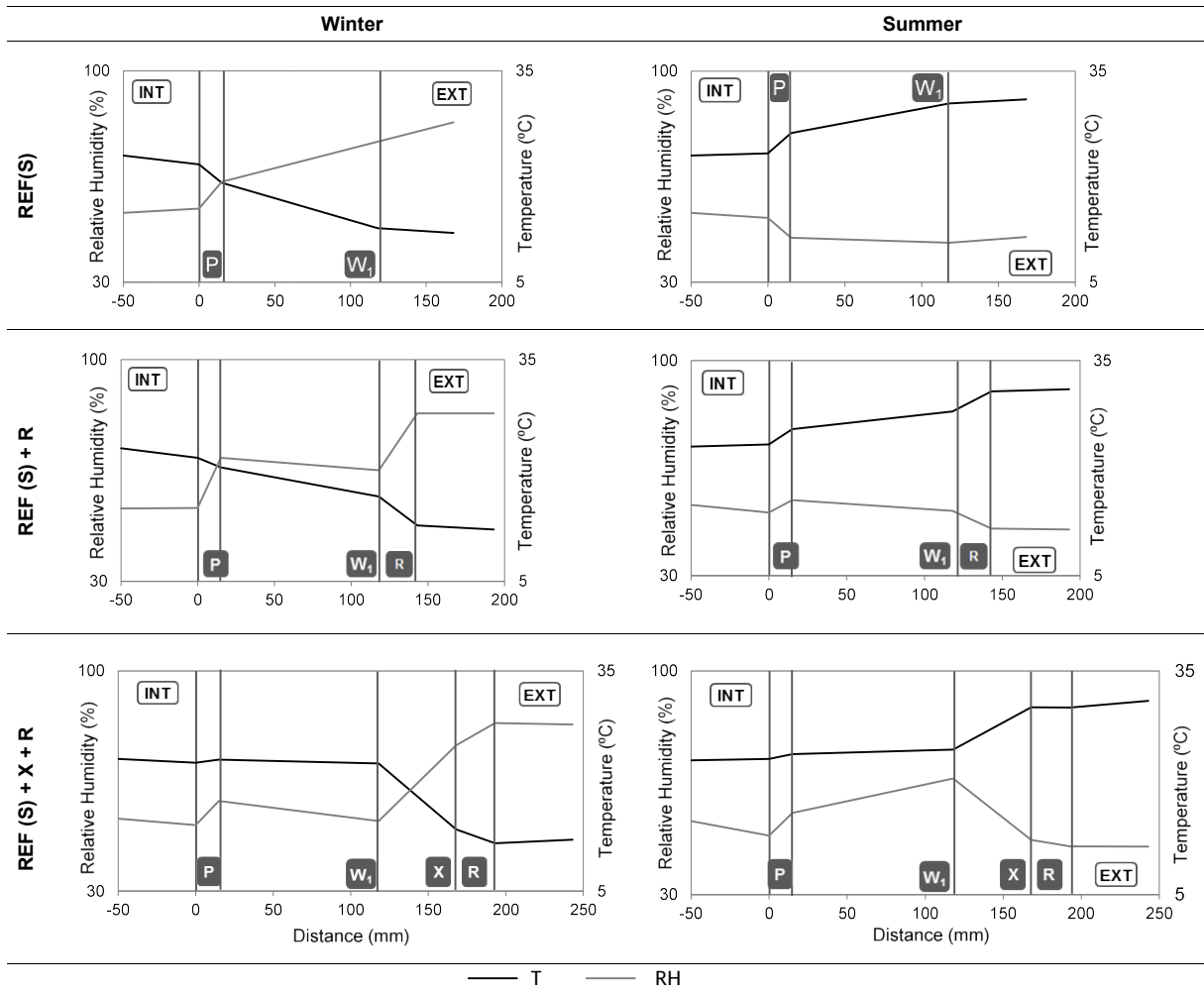


Fig. 3 Temperature and relative humidity cross-section of single walls in steady-state winter and summer scenarios

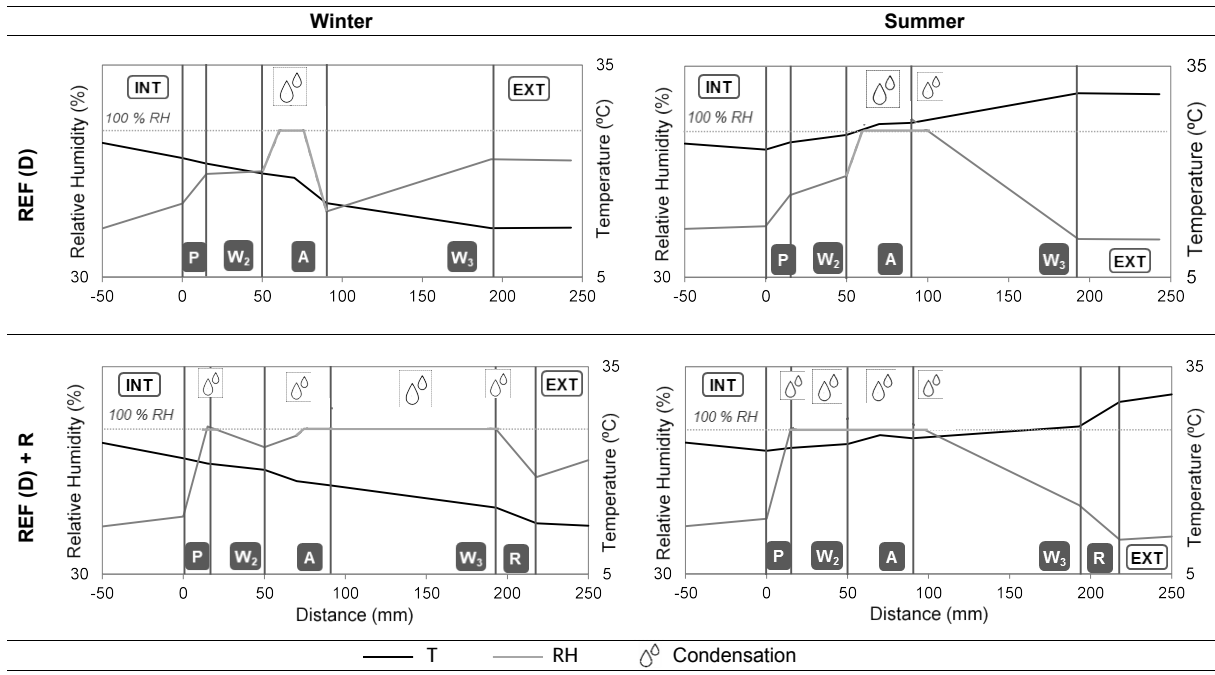


Fig. 4 Temperature and relative humidity cross-section of double walls in steady-state winter and summer scenarios

Table 1 Materials' Properties

		Plaster (P)	Perforated Brick (VPB) ^a	Solid Brick (SB) ^a	Frogged Brick (FB) ^a	Insulation Board (X) ^a	Render (R)
Thickness	mm	15	103	35	103	50	25
ρ	Kg/m ³	1000	1600	2000	1900	30	1800
μ (dry/wet)	-	70 / 6	100 / 50	100 / 50	100 / 50	-	- / 3.40
λ	W/m K	0.24	0.72	0.87	0.51	0.022	0.19
c_p	J/kg K	1000	1000	1000	1000	1400	1000
α	10 ⁻⁷ m ² /s	2.40	4.50	4.35	2.68	5.24	1.06
ρ - Bulk density			μ - Moisture-dependent water vapor diffusion resistance factor				
λ - Thermal conductivity			c_p - Specific heat		α - Thermal diffusivity		

^a Nominal values, provided by the manufacturers.

Table 2 Laboratory measured thermal parameters in winter and summer scenarios

		REF (S)	REF (S) + R	REF (S) + X+ R	REF (D)	REF (D) + R	
WINTER	ΔT	° C	-9.06	-9.23	-11.39	-9.86	-9.36
	HF	W /m ²	-50.41	-30.19	-2.20	-20.73	-18.46
	Λ	W/m ² K	5.56	3.27	0.19	2.10	1.97
	$t_{s,\Delta T}$	h	2.83	6.00	2.00	3.83	3.17
	$t_{s,HF}$	h	4.50	9.00	2.33	8.67	1.67
	CR	-	No	No	No	Yes	Yes
SUMMER	ΔT	° C	6.87	7.39	7.08	8.00	7.11
	HF	W /m ²	31.96	18.93	5.19	13.89	6.19
	Λ	W/m ² K	4.65	2.56	0.73	1.74	0.87
	$t_{s,\Delta T}$	h	1.50	2.00	2.33	6.50	6.00
	$t_{s,HF}$	h	6.00	12.83	6.00	6.67	18.00
	CR	-	No	No	No	Yes	Yes
ΔT – Temperature difference		HF – Density of heat flux rate		Λ – Thermal conductance			
$t_{s,\Delta T}$ – Stabilization time of ΔT		$t_{s,HF}$ – Stabilization time of HF		CR – Condensation risk			

Table 3 Temperature, relative humidity and heat flux stabilization time of single and double walls in winter and summer scenarios

		REF (S)		REF (S) + R		REF (S) + X+ R		REF (D)		REF (D) + R		
		HF		HF		HF		HF		HF		
		Time (h)		9.00		2.33		8.67		1.67		
		T	RH	T	RH	T	RH	T	RH	T	RH	
WINTER	S _i	h	3.00	1.33	5.50	4.83	4.33	4.00	7.50	7.50	0.67	1.00
	P- W ₁	h	3.50	1.67	9.67	8.00	0.50	4.67	-	-	-	-
	W ₁ - R	h	-	-	10.33	6.33	-	-	-	-	-	-
	W ₁ - X	h	-	-	-	-	2.67	4.00	-	-	-	-
	X - R	h	-	-	-	-	5.33	13.83	-	-	-	-
	P- W ₂	h	-	-	-	-	-	-	9.50	9.33	1.67	10.83
	W ₂ - A	h	-	-	-	-	-	-	11.00	x	8.33	6.67
	A	h	-	-	-	-	-	-	12.33	9.83	3.17	0.67
	A- W ₃	h	-	-	-	-	-	-	13.83	5.67	4.33	3.00
	W ₃ - R	h	-	-	-	-	-	-	-	-	11.50	9.17
	S _e	h	2.00	3.00	6.33	4.33	2.67	3.17	8.33	7.50	7.00	5.33
		HF		HF		HF		HF		HF		
		Time (h)		12.83		6.00		6.67		18.00		
		T	RH	T	RH	T	RH	T	RH	T	RH	
SUMMER	S _i	h	4.50	9.50	6.50	6.00	0.00	0.00	6.50	3.67	12.00	6.00
	P- W ₁	h	7.00	14.50	11.00	17.67	7.83	18.00	-	-	-	-
	W ₁ - R	h	-	-	12.00	10.33	-	-	-	-	-	-
	W ₁ - X	h	-	-	-	-	10.17	12.00	-	-	-	-
	X - R	h	-	-	-	-	3.00	11.83	-	-	-	-
	P- W ₂	h	-	-	-	-	-	-	12.50	7.50	16.00	4.17
	W ₂ - A	h	-	-	-	-	-	-	12.67	x	18.50	7.17
	A	h	-	-	-	-	-	-	11.00	11.67	24.00	10.50
	A- W ₃	h	-	-	-	-	-	-	11.00	1.33	24.00	x
	W ₃ - R	h	-	-	-	-	-	-	-	-	22.33	x
	S _e	h	3.00	18.00	6.33	6.00	2.17	4.67	2.67	3.33	12.00	4.83
T – Temperature		RH – Relative Humidity				HF – Density of heat flux rate						
P - One coat universal plaster		R - Lime-cement mortar				X - PIR insulation board						
W ₁ - Perforated brick layer		W ₂ - Solid brick layer				W ₃ - Frogged brick layer						
A - No ventilated air cavity		S _i – Surface interior				S _e – Surface exterior						